

# Non-local Electroweak Baryogenesis

## Part I : Thin Wall Regime

Michael Joyce<sup>†</sup>

Tomislav Prokopec<sup>†</sup>

and

Neil Turok<sup>†</sup>

Joseph Henry Laboratories

Princeton University

Princeton, NJ 08544.

### Abstract

We investigate ‘non-local’ schemes for baryogenesis at a first order electroweak phase transition, in which the effects of a  $CP$  violating condensate on the bubble wall propagate into the unbroken phase where the sphaleron rate is unsuppressed. Such a condensate exists in multi-Higgs extensions of the standard model, and may exist due to an instability in the minimal standard model. In this paper we first discuss the general problem of determining the  $CP$  violating perturbations, distinguishing two regimes (quantum and classical). We then give an analytic treatment of quantum mechanical reflection in the thin wall regime, in which interactions with the plasma can be neglected as a particle propagates across the wall. We focus on leptons because of their much weaker coupling to the plasma. We argue that they are likely to be accurately described by this calculation, but quarks are not. The relative magnitude of the baryon asymmetry produced for different fermions depends on their relative Yukawa couplings (*not* their zero temperature masses), their transport properties and their interactions. We calculate the baryon asymmetry for various parameter ranges and conclude that asymmetries comparable with observations

---

<sup>†</sup> e-mail: joyce@nxth01.cern.ch, tomislav@hepth.cornell.edu,  
neil@puhep1.princeton.edu

can be generated.

Revised: October 1995

## 1. Introduction

Almost twenty years passed before it was realized that the conditions stated by Sakharov for the dynamical generation of the baryon asymmetry in the universe were actually satisfied in the standard Weinberg-Salam model [1]. The required baryon number violating processes arise from the chiral nature of the theory and the topology of the vacuum, as encoded in the chiral  $SU(2)_L$  anomaly [2]. C and CP violation are built into the standard model, and Sakharov's final ingredient, a departure from thermal equilibrium, is believed to be provided by the first-order nature of the electroweak phase transition.

Despite the fact that the minimal standard model has all of Sakharov's ingredients, it has proven difficult to use it to produce the required asymmetry. The main obstacle to its success is the very small CP violation in the KM matrix. A second problem is ensuring that the baryon number violating processes are suppressed after the phase transition - this translates into a rather low upper bound on the Higgs mass  $M_H \leq 35-80$  GeV, potentially in conflict with the experimental lower bound. The exact constraint is still rather uncertain, because it relies on the details of the finite temperature effective potential, which has only recently begun to be seriously studied [3]; [4], [5], [6], [7]. A further problem for baryogenesis in the minimal standard model is that for the observed top quark mass, unless the Higgs is relatively heavy,  $M_H \geq 130$  GeV, the *zero* temperature effective potential is unbounded from below, and this leads to an unacceptable instability [8].

One notable recent attempt to elaborate a minimal standard model mechanism is that of Farrar and Shaposhnikov [9], who make use of subtle finite temperature effects on the reflection of quarks from the bubble walls formed at the phase transition. This calculation has been argued in [10] and [11] to greatly overestimate the baryon asymmetry, because it neglects the imaginary part of the quark self-energy. A suggestion as to how CP violation could be amplified in the minimal standard model was made by Nasser and Turok [12]. The idea here is that CP could be spontaneously broken by the formation of a  $Z$  boson condensate on the bubble wall, and that the competition between macroscopic domains could enhance the difference in free energy between the different sign condensates.

The most clearly viable mechanisms elaborated to date work with extensions of the standard model, the simplest such extensions being those where there are extra Higgs fields. From a particle physics standpoint this requires little justification and readily provides the extra source of CP violation which seems necessary. Following suggestions of Shaposhnikov [13], and McLerran [14], Turok and Zadrozny [15] showed how this could work in multi-Higgs extensions of the standard model. In these theories there is a CP odd Higgs field phase which changes in a definite manner in bubble walls as the Higgs fields 'roll' from the unbroken to the broken symmetry vacuum. This phase couples to the anomaly through a triangle diagram producing a biasing of the anomalous processes [16], [17]. As the bubble walls propagate through the universe they leave behind a trail of baryons.

Cohen, Kaplan and Nelson (CKN) proposed two potentially more efficient mechanisms in the same theories, 'spontaneous' baryogenesis [18], and the 'charge transport' mechanism [19]. The 'spontaneous' mechanism was an application of an earlier idea employing GUT baryon number violation [20], the charge transport mechanism developed an idea involving a lepton number violating phase transition arranged to occur at the electroweak scale [21]. Dine et. al. [22] also gave a discussion of 'spontaneous' baryogenesis employing

electroweak baryon number violation in general terms involving theories with a higher energy scale. An interesting extension of these ideas is the work of Comelli et. al. who showed that finite temperature effects can cause the spontaneous violation of CP in the minimal supersymmetric standard model. Bubbles of both CP types nucleate, but any small explicit CP violation is greatly amplified because it comes into the exponent of the bubble nucleation rate [23].

CKN originally argued that ‘spontaneous’ baryogenesis would work well in multi-Higgs theories in the ‘adiabatic’ limit of slow and thick walls. A phase redefinition of the quark fields was used to identify a term in the Lagrangian which acts like a potential for fermionic hypercharge on the bubble wall where the relative phase of the Higgs fields is changing. CKN calculated the local thermal equilibrium established in this background, with certain ‘fast’ perturbative processes allowed to equilibrate, and showed that it resulted in a non-zero baryon number violation rate. In [24] however we argued that inappropriate constraints were imposed on global conserved charges in this calculation and that the thermal equilibrium which is in fact approached has zero baryon violation. A correct calculation of this effect involves finding the departure from this equilibrium induced by the motion of the wall, determining how the motion of the wall competes with transport processes which tend to restore it to equilibrium. In the limit of perfect particle transport we showed that the system approaches the thermal equilibrium with zero baryon production. Dine and Thomas [25] have also questioned whether it is correct to treat the system as described by a fermionic hypercharge potential, pointing out that this manifestly does not have the correct behaviour as the Higgs vev vanishes.

The second mechanism suggested by CKN, the ‘charge transport’ mechanism, was argued to apply in the case of thin bubble walls. The reflection of fermions off the bubble walls in a CP violating way leads to the injection into the unbroken phase of particle asymmetries which then bias the baryon number violating processes in this region. In [21] this mechanism was applied to a heavy (4th generation) majoron neutrino with explicit CP violation in Yukawa couplings. Subsequently [21] CKN showed how in a similar way the effect of CP violation in the Higgs sector in a multi-Higgs extension of the standard model could be mediated into the unbroken phase by reflected top quarks, and sizeable baryon asymmetries produced. These calculations were supposed to apply only to thin walls because the ‘quantum mechanical’ reflection effect was taken to be suppressed when the wall is thicker (i) than the quark mean free path, because of scattering *or* (ii) than the Compton wavelength, because of the validity in this limit of the WKB approximation.

As pointed out by CKN this second mechanism has a great advantage over previously suggested ones. It is ‘non-local’ in the sense that the CP violation and baryon number violation are separated from one another. The effect of the CP violation on the wall can be propagated away from the wall into the unbroken phase, where the baryon number violating processes are unsuppressed.

In this and an accompanying paper [26] we will consider these ideas in a framework which makes clear their relation to one another. Essentially there is just one physical mechanism: on the bubble walls a background field is turned on which affects both the dynamics and the interaction rates of the fermions. Our calculations will apply both to the case of a two doublet extension of the standard model and the case of a  $Z$  boson

condensate in the standard model. We will find that the property of non-locality can in fact be generalized to the case of thick walls and used to greatly enhance the baryon asymmetry in that limit. Corresponding to the reflection in the thin wall case there is a classical force on the wall which perturbs the particle densities on and in front of the wall, as well as a ‘spontaneous’ baryogenesis effect, albeit in a guise consistent with the criticisms of this mechanism in its original form. In the thin wall case we carry out new analytic calculations which take into account a problem in the original calculation pointed out in [24]. We develop a new analytic diffusion formalism in which all the distributions are determined dynamically. We concentrate on the case of leptons emphasizing that they are very efficiently transported into the unbroken phase and are likely to be best described by this calculation for typical wall thicknesses.

The structure of the paper is as follows. In the next section we discuss  $B$  violation in the local thermal equilibrium situation which is taken to pertain around and on the wall during the phase transition and in particular we emphasize that total left-handed fermion number should be thought of as the driving force for  $B$  violation. In section 3 we discuss the general problem of the dynamics of particles in the background of a CP violating bubble wall. We discuss how the previously explored quantum mechanical reflection has in fact a very non-trivial classical limit. This suggests a quite different approach to the problem of modelling the response of the plasma to the CP violating background when scattering on the wall must be taken into account. The rest of the paper is then concerned with the thin wall regime and this other ‘classical’ calculation is deferred to the accompanying paper [26]. In section 4 we calculate the flux injected by reflection off the wall. In Section 5 we describe our calculations of the propagation of the injected flux into the unbroken phase, and give the derivation of a set of coupled equations for the particle species which describes the diffusion and decay of the injected asymmetries. In section 6 we solve these equations and calculate the baryon asymmetries produced in various regimes. In section 7 we discuss the issue of screening. While the diffusion formalism allows for a complete treatment of screening, this addition significantly complicates the analysis, and so for the most part we ignore it. We attempt to justify this in Section 7, where we give a qualitative argument that including screening effects would alter our results at most by a factor of order unity. In section 8 we calculate the baryon to entropy ratio and discuss our results, comparing the cases of injected quark and lepton fluxes. In the concluding section we summarize very briefly and point out directions for further work.

## 2. Baryon Number Violation

The departure from thermal equilibrium which is required for dynamical baryogenesis occurs as the true vacuum bubbles sweep through the false vacuum. We shall in this and the accompanying paper describe this departure from equilibrium with space-time dependent chemical potentials for each particle species. Whilst the perturbations are not in general of this simple form, in many circumstances as we shall argue in detail below, thermalisation towards such a constrained local thermal equilibrium are rather efficient, and this allows for a greatly simplified description of the baryogenesis process.

The chemical potentials for the different particle species are fixed by the local values of the charges conserved by ‘fast’ processes which have time to equilibrate. Other ‘slow’ processes (such as baryon number violation) remain out of equilibrium over the relevant

timescales. In these circumstances the rate at which a charge  $X$  conserved by the ‘fast’ processes moves towards its equilibrium value is given by

$$\dot{X} = -\bar{\Gamma} \frac{\Delta F}{T} \Delta X \quad (1)$$

where  $\bar{\Gamma}$  is the equilibrium rate for the process which violates  $X$ ,  $\Delta F$  is the difference in free energy between the two states (in which the process is in and out of equilibrium respectively) and  $\Delta X$  is the amount by which  $X$  changes in the process. This equation can be derived simply from detailed balance considerations. Applying this to the case of  $B$  violation one has simply

$$\dot{B} = -\bar{\Gamma}_s \frac{\mu_B}{T} \quad (2)$$

where  $\bar{\Gamma}_s$  is the sphaleron rate (per unit volume per unit time)<sup>†</sup> and  $\mu_B$  is the chemical potential for  $B$ . CKN have phrased the problem in these terms and set out in each of their scenarios to show that  $\mu_B$  is non-zero on or in front of the wall.

It is useful to emphasize another form of this equation. Consider a process  $\nu_i n_i \leftrightarrow 0$  (in notation where, for example,  $2n_1 + n_2 \leftrightarrow 3n_3$  has  $\nu_1 = 2$ ,  $\nu_2 = 1$  and  $\nu_3 = -3$ ) for which the rate is  $\Gamma$ . If the particles are in local thermal equilibrium with chemical potential  $\mu_i$  then from (1)

$$\dot{n}_i = -\frac{\bar{\Gamma}}{T} (\nu_i \Sigma_j \nu_j \mu_j). \quad (3)$$

Using the fact that the sphaleron processes are  $t_L t_L b_L \tau_L \leftrightarrow 0$  and  $t_L b_L b_L \nu_L \leftrightarrow 0$  (for a single fermion family with obvious notations) we can write find

$$\dot{B} = -\frac{\bar{\Gamma}_s}{2T} (3\mu_{t_L} + 3\mu_{b_L} + \mu_{\tau_L} + \mu_{\nu_L}) \quad (4)$$

or, if there are  $N_F$  families,

$$\dot{B} = -N_F \frac{\bar{\Gamma}_s}{2T} \Sigma_i (3\mu_{t_L}^i + 3\mu_{b_L}^i + \mu_{\tau_L}^i + \mu_{\nu_L}^i) \quad (5)$$

where the sum is over the families. Here the chemical potentials stand for the *difference* between particle and anti-particle chemical potentials. Equation (5) tells us that what we must do in order to calculate  $B$  violation is follow how the densities of *left-handed fermions* and their anti-particles are perturbed. In their work on charge transport baryogenesis CKN have presented hypercharge or a charge  $X$  ‘orthogonal’ to it as the quantity driving baryogenesis. As discussed in [24] this emphasis is misplaced - it is clear from (5) that one can have non-zero hypercharge without any  $B$  violation, and  $B$  violation with zero hypercharge. In the approach we describe in these papers all charges will be determined dynamically and we will always use the formula (5) directly.

---

<sup>†</sup> We will use a bar over rates to denote rates per unit volume.

In the case that the fermions are massless there is a simple relation between the chemical potential and the perturbation to the number density: for particles  $\delta n_i = \mu_i T^2/12$ , and the opposite for antiparticles. In this case equation (5) becomes

$$\dot{B} = -6N_F \frac{\bar{\Gamma}_s}{T^3} (3B_L + L_L) \quad (6)$$

where  $B_L$  and  $L_L$  are the total left-handed baryon and lepton number densities respectively. The factor of 3 is just a result of the definition of baryon number (i.e.  $\frac{1}{3}$  per quark) - the quantity in brackets is just the total left-handed fermion number.

We can use (6) to comment on the role of strong sphaleron processes. Giudice and Shaposhnikov have pointed out [27] that if one treats these as ‘fast’ in the constraint calculations carried out by CKN (as they argue one should) one finds that the result is that there is no  $B$  violation. One must then go to the mass induced corrections to (6) to get a non-zero result. This result has a simple explanation. In all these calculations  $B$  and  $B - L_L$  are constrained to be zero. Also, since strong sphalerons couple right and left-handed baryons as  $t_L \bar{t}_R b_L \bar{b}_R \dots \leftrightarrow 0$  it follows from (3) that the sum of the chemical potentials of left handed baryons is equal to that of right-handed baryons if this process is in thermal equilibrium. In the massless limit this leads to the relation  $B_L = B_R$  which, together with the constraints  $B = 0 = L_L$ , immediately gives  $\dot{B} \propto 3B_L + L_L = 0$  from (6). It is clear however that if one injects net left-handed lepton number into the system that this argument does not apply. We defer a full discussion of this issue to the appropriate point below.

Now we turn to the analysis of how CP violation on the wall perturbs the left-handed fermion number on and in the vicinity of the wall. This then drives  $B$  violation according to equation (5).

### 3. Particle Dynamics on a CP-violating Wall

We are interested in the effects of  $CP$  violating condensates on the bubble wall. To date, the two simplest suggestions for this are the relative phase of two Higgs fields in a two-Higgs theory [15], [16], or the longitudinal  $Z$  boson [12]. Our analysis will include both of these possibilities. The former case is conceptually simpler - if there is explicit  $CP$  violation in the Higgs potential, the relative phase of the two Higgs fields is a  $CP$  odd field, which changes in a definite manner as the Higgs fields change from zero in the unbroken symmetry phase to their final nonzero values in the broken symmetry phase [15], [16]. The latter case relies instead on an instability which may occur if the top quark mass is sufficiently large [12].

Let us try first to define the relevant physical degrees of freedom. We can use the  $SU(2)$  symmetry to pick a gauge in which the background classical solution provided by the wall is  $\varphi_1 = \frac{1}{\sqrt{2}}(0, v_1 e^{i\theta_1})$ ,  $\varphi_2 = \frac{1}{\sqrt{2}}(0, v_2 e^{i\theta_2})$ . We assume that at all stages during the phase transition electromagnetic  $U(1)$  symmetry is unbroken. We could with a gauge choice set  $\theta_1$  or  $\theta_2$  to zero, but it is instructive not to do so, in order to clearly see how the (gauge invariant)  $CP$ -odd relative phase  $\theta = \theta_1 - \theta_2$  emerges. It is clear that since the relative phase loses its meaning when the vevs vanish, *all physical effects which depend on the relative phase of the two Higgs fields must vanish as either Higgs vev does*. We shall see that this condition is met in a somewhat nontrivial manner.

The physical degrees of freedom in the broken phase are fluctuations in the two vevs,  $\delta v_1$  and  $\delta v_2$ , in the relative phase  $\theta$ , and the charged Higgs fluctuations  $\varphi^+$ . Diagonalising the Higgs kinetic terms we find

$$\begin{aligned} |\mathcal{D}\varphi_1|^2 + |\mathcal{D}\varphi_2|^2 &= \frac{1}{2} \frac{v_1^2 v_2^2}{v^2} (\partial_\mu(\theta_1 - \theta_2))^2 + \frac{1}{2} v^2 \left[ \frac{g}{2} Z_\mu - \left( \frac{v_1^2 \partial_\mu \theta_1 + v_2^2 \partial_\mu \theta_2}{v^2} \right) \right]^2 \\ &\equiv \frac{1}{2} \frac{v_1^2 v_2^2}{v^2} (\partial\theta)^2 + \frac{1}{2} v^2 \left( \frac{g}{2} Z_{GI} \right)^2 \end{aligned} \quad (7)$$

where  $v^2 = v_1^2 + v_2^2$  and  $g^2 = g_1^2 + g_2^2$ . We ignore for now the kinetic terms for  $v_1$  and  $v_2$ , the charged  $W$  bosons and the charged Higgs fluctuations  $\varphi^+$  (we shall return to the latter below).  $Z_\mu$  is the usual (gauge variant) expression in terms of  $W_\mu^3$  and  $B_\mu$ . Both  $\theta$  and  $Z_\mu^{GI}$  are gauge invariant, and we take them as our definition of the  $CP$  violating condensate field and the  $Z$  field respectively.

Assume for simplicity that only  $\varphi_1$  couples to the fermions via Yukawa terms. The phase of the Higgs field  $\theta_1$  can be removed by performing a  $T^3$  (or hypercharge  $Y$  - the two are equivalent since  $Q = T^3 + Y$  is an unbroken exact symmetry) rotation on the fermions, at the cost of introducing a coupling  $\partial_\mu \theta_1 T^3$ , i.e. a pure gauge potential for  $T^3$  into the fermion kinetic terms. Let us see what effect this has. We may combine the  $\partial_\mu \theta_1 T^3$  potential with the coupling to the  $Z_\mu$  field to find

$$\bar{\psi} i \gamma^\mu (\partial_\mu - i g_A \tilde{Z}_\mu \gamma^5) \psi - m \bar{\psi} \psi \quad (8)$$

where  $g_A = +g/4$  for up-type quarks and (left-handed) neutrino, and  $g_A = -g/4$  for down-type quarks and leptons, and

$$g_A \tilde{Z}_\mu = g_A Z_\mu^{GI} - \frac{1}{2} \frac{v_2^2}{v_1^2 + v_2^2} \partial^\mu \theta \quad (9)$$

where  $g_A = \frac{1}{4}g$ . The vector contribution from the  $T^3$  potential does not appear in (8) for the following reason. We treat the wall as planar, and assume it has reached a static configuration in the wall rest frame, with the background scalar fields being functions only of  $z$ , and the field  $\tilde{Z}_\mu = (0, 0, 0, Z(z))$  being pure gauge. We can then remove the vector term using the remaining unbroken anomaly-free vector symmetries: A hypercharge rotation leaves a vector piece which couples each fermion in proportion to  $B - L$ , which can itself be removed by the appropriate  $B - L$  rotation. Precisely the charge  $g_A$  as given in (8) is the linear combination  $[\frac{1}{2}(T_3 - Y) + \frac{1}{4}(B - L)]g$ . The remaining axial term *cannot* be gauged away, and (as we shall see) has a real physical effect.

Let us briefly mention how the calculation is done in unitary gauge. In this gauge, the massive gauge bosons are just the original gauge bosons i.e. the Goldstone modes that would have been ‘eaten’ by the gauge bosons are set zero. This condition is just that the gauge current corresponding to each broken symmetry (with generator  $T^a$  and corresponding gauge field  $W_\mu^a$ ), give by  $\partial\mathcal{L}/\partial W_\mu^a$  be set zero at zero  $W_\mu^a$ . Then the Lagrangian  $\mathcal{L}$  is quadratic in  $W_\mu^a$ , and there is no need for any ‘eating’ to occur. In our case, this condition is just  $i\varphi^*(1 - \sigma_3)\partial_\mu\varphi + \text{h.c.} = 0$ , or  $v_1^2\partial\theta_1 = -v_2^2\partial\theta_2$ . Then  $Z_\mu^{GI} = Z_\mu$ , and it is clear that



the fermion rotation by  $\theta_1 T^3$  induces a potential of exactly  $\partial_\mu \theta_1 T^3$  into the fermion kinetic terms. After dropping the vector coupling, this agrees with (9).

In describing the rotations required to bring the Lagrangian to the form of (8) we did not consider the Higgs fluctuations. As remarked by Dine and Thomas [25], a  $T^3$  rotation such as the one we performed to remove the phases from the fermion mass terms introduces some  $\theta_1$  dependence into the Higgs-fermion interaction terms. To remove this one has to perform a rotation on the Higgs fields, which introduces some dependence on  $\partial_\mu \theta$  in the Higgs kinetic terms. In the limit that the vevs vanish this rotation is just a  $T^3$  rotation of the Higgs fields (or  $T^3 - Y$  when we perform the subsequent hypercharge rotation to remove the vector term in the fermionic Lagrangian), and the induced term simply a coupling to the field  $\tilde{Z}_\mu$  which makes up the remaining piece of the pure gauge potential. The  $g_A$  charges corresponding to the form in (8) are 0 and  $-g/2$  for the charged and neutral Higgs components respectively. (so that  $g_A$  charges which are just proportional to a linear combination of  $T^3 - Y$  and  $B - L$  charges are conserved in any interaction).

Let us consider a little further the Higgs sector when the vevs are not zero. The  $T^3$  rotation on the fermions then induces a  $\theta_1$  dependence in, for example, the charged Higgs-fermion interaction term  $\varphi^+ \bar{t}_L b_R$ . We now define the charged Higgs fluctuations in unitary gauge. With the notation  $\varphi_1 = (\varphi_1^+, v_1/\sqrt{2})$  (i.e. absorbing the phase into  $v_1$ ), and similarly for  $\varphi_2$ , one finds the unitary gauge condition is

$$\varphi_1^{+*} \partial_\mu v_1 + \varphi_2^{+*} \partial_\mu v_2 = \partial_\mu \varphi_1^{+*} v_1 + \partial_\mu \varphi_2^{+*} v_2 \quad (10)$$

Now we write the kinetic terms for the Higgs fluctuations:

$$K = |\partial_\mu \varphi_1^+|^2 + |\partial_\mu \varphi_2^+|^2 \propto |\partial_\mu \varphi_1^{+*} v_1 + \partial_\mu \varphi_2^{+*} v_2|^2 + |\partial_\mu \varphi_1^{+*} v_2 - \partial_\mu \varphi_2^{+*} v_1|^2 \quad (11)$$

We shall see how a potential for  $T^3$  emerges in the Higgs sector in a certain approximation, more restrictive than in the case of the fermions. If we drop derivatives of  $|v_1|$  and  $|v_2|$ , then we find upon substituting (10) for the first term in (11) that it is quadratic in  $\partial_\mu \theta_1$  and  $\partial_\mu \theta_2$ . Let us make the approximation of ignoring such terms. If we now rotate the fermions by  $e^{i\theta_1 T^3}$  to remove the phase from the fermion mass term, we must rotate  $\varphi_1^+$  by the same rotation to remove the phase from the Higgs-fermion interactions, and  $\varphi_2^+$  by the same rotation to remove the phase from the Higgs-Higgs couplings. Setting  $\varphi_1^+ = f_1 e^{-i\theta_1}$   $\varphi_2^+ = f_2 e^{-i\theta_1}$ , we find the second term in (11) becomes

$$K \propto |\partial_\mu f_1^* v_2 - \partial_\mu f_2^* v_1 + i\partial_\mu \theta_1 (f_1^* v_2 - f_2^* v_1)|^2 \simeq |\partial_\mu \chi + i\chi \partial_\mu \theta_1|^2 \quad (12)$$

where  $\chi = f_1^* v_2 - f_2^* v_1$  is the physical charged Higgs excitation. Thus, in this approximation, one really can describe the effects of  $\partial_\mu \theta_1$  as a  $T^3$  potential for charged Higgs excitations (this was originally argued to be true by Dine and Thomas [25]).

One other assumption we made in deriving (8) was that only a single Higgs field coupled to the fermions. If both Higgs fields couple to the fermions we can carry out the same procedure to remove all the phases from the Yukawa terms involving one Higgs field,

but are left then with the phase  $\theta$  in the Yukawa terms involving the second Higgs field. There are alternative ways of writing this Lagrangian - we can choose where to put the relative phase but cannot get rid of it and make all the mass terms real. In what follows we will always consider cases where at most a single Higgs field couples to any given fermion, so that in studying the dynamics of a given fermion in the CP violating background we can always take its Lagrangian to be of the form (8) with a real mass term.

So what is the effect on the dynamics of fermions of turning on an axially coupled pure gauge field in the presence of a mass? And how are the distributions of the particles in the plasma affected by this background? We first consider the dynamics of a free fermion described by the Lagrangian (8). Because of translation invariance in the direction perpendicular to  $z$ , the momentum  $p_\perp$  is a constant of the motion. With an appropriate Lorentz transformation, this may be set equal to zero and the problem becomes one dimensional. With the ansatz  $\psi \sim \exp -i\hat{E}t$ , the Dirac equation can be broken into two equations, one coupling the first and third components of  $\psi$ , and a second coupling the other two:

$$i\partial_z \xi_\pm = \begin{pmatrix} \hat{E} \pm g_A Z & m \\ -m & -(\hat{E} \pm g_A Z) \end{pmatrix} \xi_\pm \quad S^z = \pm \frac{1}{2} \quad (13)$$

We are working here in the chiral representation to follow the convention of CKN in [21]. The energy  $\hat{E}$  here equals  $\sqrt{E^2 - p_\perp^2}$  in the original Lorentz frame. What (13) describes is the coupling of ingoing left-handed fermions to outgoing right-handed ones and vice versa. For anti-particles the same applies, except that the signs are switched i.e. left-handed particles and their anti-particles (which are right-handed) see opposite signs for the axial field. Since left-handed fermions and their anti-particles are affected oppositely we have in principle a way of generating a disturbance in left handed fermion number, which should source baryon number as discussed in section 2.

This is precisely the effect identified by CKN in the ‘charge transport’ mechanism. Once one notes that the reflection from the wall is CP violating one must simply calculate the injected fluxes and determine how they bias baryon number violation. Emphasis has thus been placed on the calculation of quantum mechanical reflection and transmission asymmetries. We will discuss in detail in section 8 the criterion for the validity of these calculations in which the fermions are treated as free particles in their interaction with the wall. Roughly the criterion is that the thickness of the wall  $L_w$  be much less than the mean free path  $\lambda_{mfp}$  of the fermions. As the wall becomes thicker  $L_w \sim \lambda_{mfp}$  strong scattering effects must be taken into account. Because CP violating reflection has been understood, for reasons which will be explained below, as a quantum mechanical effect it has been assumed that it is washed out in the limit  $L_w \gg \lambda_{mfp}$ . In the next section we discuss these reflection calculations, pointing out that there is a non-trivial WKB result which leads to quite a different conclusion and points the way to a new calculation of the thick wall case in which scattering of the fermions as they cross the wall is taken into account.

### 3.1 Two Calculations of Reflection Coefficients

As discussed in section 2 the quantity of interest in to baryon production is the difference in particle minus anti-particle distributions. We thus focus on calculating the difference in the reflection probabilities of particles of a given chirality and their antiparti-

cles, since this is the quantity that will enter the calculation (in section 4) of the currents injected into the unbroken phase.

**(i) Case 1 : Quantum Mechanical**

In Appendix A we derive an expression for the difference  $\mathcal{R}$  in the reflection coefficients (*i.e.* probabilities) of particles and anti-particles. For left-handed particles  $L$  the result is

$$\mathcal{R}(p_z) \equiv R_{L \rightarrow R} - R_{\bar{L} \rightarrow \bar{R}} = -\frac{4t(1-t^2)}{|m_f|} \int_{-\infty}^{\infty} \mathcal{I}m[m(z)m_f^*] \cos(2p_z z) dz \quad (14)$$

where  $m_f$  is  $m(-\infty)$ , the mass of the fermion in the broken phase, and  $t = \tanh\theta$  where  $\tanh 2\theta = |m_f|/|p_z|$ . Here  $p_z$  denotes the value of the momentum at infinity (in the unbroken phase). Henceforth we shall set the phase of the fermion mass  $m_f$  to be *zero* in the broken phase. Equation (14) is valid for any wall profile and gives the leading term in an expansion in  $L_w m_f$ , where  $L_w$  is the thickness of the wall. Only when this expansion is valid is there a range of incident momenta which are both not totally reflected ( $p_z > m_f$ ) and also non-WKB ( $p_z < L_w^{-1}$ ). It is because of this that we refer to it as the ‘quantum mechanical expansion’.

To see the effect of the cosine term in the integral we evaluate (14) for an imaginary mass of a Gaussian form :  $\mathcal{I}m[m] = m_I = \frac{m_f}{\sqrt{\pi}} \exp -(m_H z)^2$ . The result for the reflection coefficient is then:

$$\mathcal{R} = 4t(1-t^2) \frac{m_f}{m_H} \Theta_{CP} e^{-\left(\frac{p_z}{m_H}\right)^2}, \quad (15)$$

where  $\Theta_{CP}$  is defined by  $\int \mathcal{I}m[m] dz = \frac{m_f}{m_H} \Theta_{CP}$ . (15) illustrates that the effect is quantum mechanical, as it is exponentially suppressed in the WKB limit, and in the limit  $|p_z|L_w < 1$  clearly involves a non-local coherence effect across the wall in which the particle and anti-particle pick up different phases as they propagate.

This is the effect identified by CKN when they calculated the reflection coefficients numerically for a definite wall profile, and also in [28]. They found strong suppression of reflection for momenta larger than the inverse wall thickness and concluded correctly that they were seeing a phase coherence effect which would be strongly suppressed for all momenta when the effects of scatterings on the bubble wall are accounted for. Consideration of the WKB limit will now show that this analysis misses an important point.

**(ii) Case 2 : WKB Regime**

We now consider the limit in which the functions  $m$  and  $Z$  vary slowly in comparison to the Compton wavelength of the fermion. The WKB solutions to (13) then describe excitations which may be thought of as particles with definite momentum and position. They are described by the dispersion relation

$$E = \left[ p_{\perp}^2 + (\sqrt{p_z^2 + m^2} \mp g_A Z)^2 \right]^{1/2} \quad S^z = \pm \frac{1}{2} \quad (16)$$

where  $S^z$  refers to the spin of the particle in the frame where  $p_{\perp}$  vanishes. For particles incident from the unbroken phase this is equivalent to chirality. This equation only makes sense for  $m > |g_A Z|$ , and we assume this holds everywhere. If this condition is violated,

‘positive energy’ solutions can mix with ‘negative energy’ ones and one expects particle creation to occur (as in the Klein paradox). We shall not consider this possibility here.

A particle incident from the unbroken phase with momentum  $p_z(\infty) = p_\infty$  is reflected if

$$|p_\infty| < m(z) \mp g_A Z(z) \quad (17)$$

holds for any  $z$ . From (17) we can read off the difference in the reflection coefficients:

$$R_{L \rightarrow R} - R_{\bar{L} \rightarrow \bar{R}} = \begin{cases} 1, & |p_\infty| \in [m_f, \max[m(z) + g_A Z(z)]] \\ 0 & \text{otherwise} \end{cases} \quad (18)$$

(where we have assumed  $g_A Z(z)$  is positive), ignoring barrier penetration effects.

What this analysis reveals is that high  $p_z$  (i.e. WKB) particles see the axial field on the wall as producing an extra potential superimposed on the real mass barrier. This extra potential has an opposite sign for particles and anti-particles. If the shape of the extra potential is monotonic like that shown in Figure 1 this potential does not produce a difference in reflection coefficients for the ‘classical’ particles and their anti-particles. The only interesting reflection will come at low ‘quantum mechanical’ momenta for which the different phases picked up by particles and antiparticles moving in this potential causes differential reflection. However if the potential looks more like that in Figure 2 (with a bump) there will be a difference in reflection coefficients of particles and anti-particles even in the WKB limit. Thus we see that the exponential suppression we observed in (15) was a result of the particular ansatz we took for the wall profile. Similar monotonic ansatzes have been assumed by CKN and other authors [28].

Besides revealing a sensitivity to the ansatz in the calculation of the reflection coefficient, in particular that there can be non-trivial reflection of WKB particles, this discussion is of relevance to the thick wall case. The effect being treated was expected to be suppressed when scattering on the wall becomes important since it relies on a phase coherence of the particles across the wall. However the effect does not arise from such a phase coherence in the case of WKB momenta particles. As we have argued the picture appropriate to these momenta is of a (local) classical potential which is simply different for particles and anti-particles. What do we expect such a potential to give rise to? Consider the effect of turning on an electromagnetic potential in a small region of a plasma. Given a sufficient amount of time the potential will be screened - it will draw in charge - and settle down to a new thermal equilibrium in which there is a net overdensity of every particle in proportion to its electrical charge times the local value of the potential. If we consider the case in which the region moves slowly with velocity  $v$  the system will remain approximately in this thermal equilibrium but with deviations which vanish as  $v \rightarrow 0$ . We have just argued that the particles and anti-particles see an opposite potential and we thus expect that the deviations induced as the region - in this case the bubble wall - moves will reflect this difference. This should be true irrespective of whether the potential is monotonic or not. Just as in the case of an electromagnetic potential where the process of establishing the approximate equilibrium involves the electromagnetic force pulling in particles which then scatter in the potential and reach local equilibrium, there should be a force playing an analogous role. This force will be a CP violating force which will source perturbations in front of the wall much as the reflected flux does in the thin wall case.

What is the force a particle feels moving on the wall? To answer this we return to the dispersion relation (16). The velocity of the WKB particle with energy  $E$  is the group velocity

$$v_z = \frac{\partial E}{\partial p_z} = \frac{\sqrt{E^2 - p_\perp^2}}{E} \frac{p_z}{\sqrt{E^2 - p_\perp^2} \pm g_A Z} \quad S^z = \pm \frac{1}{2} \quad (19)$$

where  $p_z$  is specified by (16). A simple measure of the effect of the background is the corresponding acceleration, which may be calculated using  $\dot{p}_z = -\partial_z E$ :

$$\frac{dv_z}{dt} = -\frac{1}{2} \frac{(m^2)'}{E^2} \pm \frac{(g_A Z m^2)'}{E^2 \sqrt{E^2 - p_\perp^2}} + o((g_A Z)^2) \quad (20)$$

with  $E$  and  $p_\perp$  constants of the motion. The  $CP$  violating effect goes to zero as the mass squared does, consistent with the fact that  $Z$  may be gauged away in this limit.

In what limit is this force associated with the background likely to be important? We turn to this question in the accompanying paper [26], where we develop a new formalism to describe the effect. An accurate treatment of the ‘nonlocal’ classical effect becomes possible for thick, slow walls, where a fluid approximation may be used in order to take particle scattering on the wall into account. But in the remainder of this paper we turn to the consideration of the opposite ‘thin wall’ quantum mechanical limit, taking the fermions to propagate as free particles in the background provided by the wall.

#### 4. Injected Fluxes in the Thin Wall Regime

We first make a few comments about the physical parameters which determine the applicability of the calculations we are undertaking. In these papers we assume that the phase transition is first order and proceeds by bubble nucleation. This is supported by detailed study of the perturbative effective potential at least for rather light Higgs ( $m_H < 70 \text{ GeV}$ ) [29] and, more recently, by non-perturbative studies [7]. The parameters which are crucial to an accurate determination of the baryon asymmetry are the wall thickness  $L_w$  and the wall velocity  $v_w$ . Estimates of the bubble wall thickness from perturbative calculations in the standard model [30] indicate  $L_w \approx 2m_H^{-1} \approx \frac{10-40}{T}$ . and  $v_w \sim 0.1 - 1$ . A recent detailed study by one of us (T.P) and G. Moore [31] in the minimal standard model indicates that for Higgs masses in the range  $30 - 70 \text{ GeV}$  or so,  $v_w \sim 0.4$  and  $L_w \sim 25/T$ . If non-perturbative effects play a significant role this result could be significantly altered; a non-perturbative condensate makes the phase transition stronger with more super-cooling and hence larger  $v_w$ . Likewise in two-Higgs theories larger or smaller  $v_w$ ’s may be possible in different regions of parameter space.

The other parameters which are crucial to accurate calculations are those characterizing the particles in the hot plasma. One of our objectives in this work has been to carry out detailed calculations of diffusion constants and decay rates rather than give rough estimates of these parameters. This is particularly important because the emphasis of our work is on transport and the transport properties of quarks and leptons are quite different. An estimate of the length scale over which we can treat the fermion as free is specified by the fermion damping rate  $\gamma$  in a hot plasma [32], [10],[11]. For the slow quarks and leptons ( $p \leq gT$ ) these are

$$\gamma_q \approx 2\alpha_s T \approx \frac{T}{3.5} \quad \gamma_l \approx \alpha_w T \approx \frac{T}{30} \quad \gamma_r \approx \frac{3}{2} \alpha_w \tan^2 \theta_w T \approx \frac{T}{70} \quad (21)$$

at 100GeV, where  $\theta_w$  is the Weinberg angle, and the subscripts indicate quarks, left-handed leptons and right-handed leptons. For hard thermal particles ( $p \sim T$ ) even though the damping rates are logarithmically enhanced:  $\gamma \sim g^2 \ln(1/g^2)$ , the numerical value does not differ by much:  $\gamma_q \sim 4\alpha_s T/3$ ,  $\gamma_l \sim \alpha_w T$ . Comparing these with  $L_w$  we see that the uncertainty in  $L_w$  translates to an uncertainty about whether the fermions should be treated as free or interacting particles on the wall. It seems most likely with current understanding of the relevant parameters that leptons may be well described by a free particle treatment on the wall, but for quarks an interacting fluid approximation is needed. In this paper we shall consider the former case, in the companion paper [26] the latter.

In the context of these remarks about the likely difference between the quarks and leptons we note an interesting point related to the finite temperature properties of a two Higgs doublet model, which we believe has been overlooked in the literature. The ratio of quark and lepton masses is not in general determined by their zero temperature ratio. For example the ratio of the *top* quark mass to the  $\tau$ -lepton mass at finite temperature in the models with the couplings described above is

$$\frac{m_t(T)}{m_\tau(T)} = \frac{y_t v_1(T)}{y_\tau v_2(T)} = \frac{y_t v_1(0) v_1(T)/v_1(0)}{y_\tau v_2(0) v_2(T)/v_2(0)} = \frac{m_t(0) v_1(T)/v_1(0)}{m_\tau(0) v_2(T)/v_2(0)}. \quad (22)$$

There is no reason why the ratio of the zero temperature masses should not arise from a tuning of the *vevs* in the potential rather than from a tuning of the Yukawa couplings. If there is such a tuning we do not expect it to be respected by finite temperature corrections to the potential. Rather we expect all the finite temperature *vevs* to be of order  $T$ . Thus it is the ratio of the Yukawa couplings which is important and these can be large or small, consistently with present experimental data.

We now turn to the calculation of the injected flux in the thin wall regime which we will use in the next section to calculate the departure from thermal equilibrium in the unbroken phase. In order to get an expression for the asymmetry injected into the unbroken phase, we need to include both reflection from and transmission through the barrier. One can use CPT invariance to find the following relations between the reflection and transmission coefficients [21]

$$R_{R \rightarrow L} = R_{\bar{L} \rightarrow \bar{R}} = 1 - T_{L \rightarrow L} = 1 - T_{\bar{R} \rightarrow \bar{R}} \quad (23)$$

where the transmission coefficients are for particles incident from the broken phase. Integrating the reflection and transmission coefficients against the incident flux, and using (23) to eliminate the transmission coefficients, we arrive at an expression for the flux of injected right handed particles

$$J_i^R = \int_{p_z < 0} \frac{d^3 p}{(2\pi)^3} \frac{|p_z|}{E} (f_{\leftarrow}^L - f_{\rightarrow}^R) \mathcal{R}(p_z) \quad (24)$$

where  $f_{\leftarrow}^L$  and  $(f_{\rightarrow}^R)$  are the free particle phase-space densities (in the wall frame) of left-moving left-handed (L) and right-moving right-handed (R) particles, respectively. When the wall is at rest the term  $f_{\leftarrow}^L - f_{\rightarrow}^R$  cancels so that there is no net reflection. Taking this

term to linear order in  $v_w$ , and using the coefficients in (14), calculating again to leading order in  $\frac{m_f}{m_H}$ , and also to leading order in  $\frac{m_H}{T}$ , we find

$$J_i^L = -J_i^R = \frac{v_w}{4\pi^2} m_f^2 m_H \Theta_{CP}. \quad (25)$$

For the reflection coefficient we have taken

$$\mathcal{R}(p_z) = \begin{cases} \frac{2m_f}{p_z} \frac{m_f}{m_H} \Theta_{CP} & m_f < p_z < m_H \\ 0 & \text{otherwise} \end{cases} \quad (26)$$

In imposing the upper cut-off we assume that there is a sharp WKB suppression like that in (15). The approximation  $2t \approx \tanh 2\theta = \frac{m_f}{p_z}$  is good to leading order in  $\frac{m_f}{m_H}$  since the integrals are dominated by the larger momenta because of phase space factors.

In the WKB case, using (18), we obtain

$$J_i^L = -J_i^R = \frac{v_w}{4\pi^2} m_f^2 m_H \Theta_{CP} \eta \quad (27)$$

where we took  $g_A Z_{\max} = m_H \Theta_{CP}$ . The parameter  $\eta$  parametrises our ignorance about the exact profile and penetrability of the barrier. For a thick (impenetrable) barrier with a prominent bump such that  $\max[m(z) + g_A Z] = m_f + g_A Z_{\max}$ ,  $\eta = 1$ . In general  $\eta < 1$ . All masses in these formulae are the relevant finite temperature masses.

What is the correct ansatz for the wall profile? Although monotonic ansatzes of the type previously assumed seem plausible they are no more than that. This point is well illustrated by the calculations in [33] in which it is shown that in the standard model the backreaction of the CP violating reflection can cause an instability to the formation of a  $Z$  condensate. Without a detailed calculation of these effects it remains unclear exactly what the wall profile is.

## 5. Propagation of Injected Particle Asymmetries

We now consider the problem of how the flux calculated to be injected in the first two cases above propagates in the unbroken phase and drives  $B$  violation. The average velocity  $v_i$  relative to the wall of the injected flux can be written as

$$v_i = \frac{\int_{p_z < 0} \frac{d^3 p}{(2\pi)^3} \frac{p_z^2}{E^2} (f_{\leftarrow}^L - f_{\rightarrow}^R) \mathcal{R}(p_z)}{\int_{p_z < 0} \frac{d^3 p}{(2\pi)^3} \frac{|p_z|}{E} (f_{\leftarrow}^L - f_{\rightarrow}^R) \mathcal{R}(p_z)} \quad (28)$$

Using (14) and the same approximations as for the calculation of the flux (to leading order in  $v_w$ ,  $m_f/m_H$  and  $m_H/T$ ) we find

$$v_i = \frac{1}{4 \ln 2} \frac{m_H}{T}. \quad (29)$$

For the WKB case, using (18) and (24), the result is

$$v_i = \frac{\pi^2}{18 \zeta_3} \frac{m_f}{T} \quad (30)$$

where  $\zeta_3 \simeq 1.202$  is a Riemann zeta function. The result in both cases is roughly the ratio of the momentum in the direction of the wall of the typical reflected particle to the average thermal momentum in that direction. Note that  $v_i$  is independent of the wall velocity. The particles in this flux propagate away from the wall until they scatter. If the wall is not moving too fast they will then thermalize and diffuse until they are overtaken by the wall. Any given particle can also decay into others through decay processes and these must be taken into account.

For what range of wall velocity  $v_w$  do particles have time to thermalize before they are recaptured by the wall? Suppose that  $\tau$  is the mean time for a particle's velocity to be randomized. We take  $\tau$  to be both a thermalization time and the step time in an isotropic random walk which the particle executes once it thermalizes. Then we can estimate the mean distance a particle moves away in the direction of the wall motion in time  $t$  to be  $\sqrt{\frac{t\tau}{3}}$ . Equating this to the distance  $v_w t$  the wall moves in the same time we see that the ratio of the 'injection time'  $\tau$  to the 'diffusion time'  $t$  is approximately  $3v_w^2$ . We will restrict ourselves to the case when this ratio is small i.e.

$$v_w \ll v_s = \frac{1}{\sqrt{3}} \quad (31)$$

where  $v_s$  is the speed of sound in the relativistic plasma. We can then model the problem analytically with equations describing the diffusion and decay of a particle density perturbation sourced by an injected flux localized in a small region around the wall.

### 5.1 Calculation of Diffusion Constants

We present our calculation of the relevant diffusion constants in Appendix C. We generalize the standard treatment of this problem given in [34]. We assume the local distribution function  $f(x, p)$  to be specified by a space dependent chemical potential plus a perturbation which we fix by balancing the contribution to the change in  $f$  due to the gradient in the chemical potential against the collision term in Boltzmann's Equation. For the dominant gauge boson exchange diagrams we then arrive at expressions for the diffusion constant  $D$  which defines the relation between the diffusion current  $\vec{J}_d$  and the gradient driving it:

$$\vec{J}_d = -D\vec{\nabla}n \quad (32)$$

where  $n$  is the number density. We will give our numerical results at the appropriate point below.

### 5.2 Derivation of Propagation Equations

We now use the continuity equation to derive the equations which describe the propagation into the unbroken phase. This gives

$$\frac{dn_i}{dt} = \frac{\partial n_i}{\partial t} + \vec{\nabla} \cdot \vec{J}_i = - \sum_A \frac{\bar{\Gamma}_A}{T} \nu_i (\sum_j \nu_j^A \mu_j). \quad (33)$$

The decay term is derived using (3) and the sum over  $A$  is a sum over all the decay channels of particle  $i$ . Taking the leading (massless) term we can express this in terms of the particle



densities. In Appendix D we outline the calculation of the specific decay rates which we will need below.

Now making use of (32) and (33) and treating the wall as providing a flux  $\vec{J}_i^{inj}$  so that  $\vec{J}_i = -D_i \vec{\nabla} n_i + \vec{J}_i^{inj}$ , we find

$$D_i \partial_z^2 n_i - \partial_t n_i - \sum_A \frac{\bar{\Gamma}_A}{T} \nu_i (\sum_j \nu_j^A \mu_j) = \partial_z J_{z_i}^{inj}. \quad (34)$$

The wall can be treated in this way since it conserves particle number, simply sending equal and opposite particle number in opposite directions. It can thus be described as producing a ‘blip’ in the flux, and taking it to be constant in the wall frame, we model it as

$$J_i^{inj}(z) = \xi_i J_i^0 \delta(z - v_w t) \quad (35)$$

where  $J_i^0$  is the net reflected flux for each species  $i$ , given for example for right handed particles by equation (24). We define a parameter here called  $\xi_i$  which defines the persistence length of the current in the vicinity of the wall, and we approximate the injected current with a delta function. This is reasonable if the injected current thermalizes in a time  $\tau_{th}$  short in comparison to the time a particle spends diffusing before being recaptured by the wall - which is just the criterion (31).

Our ignorance about how the injected flux thermalizes is parametrized by  $\xi_i$ . The uncertainty in this parameter is unfortunately intrinsic to the analytic approximation we are using in taking the departure from thermal equilibrium to be modelled by a chemical potential, a form to which the injected flux does not in general conform.

Nevertheless an estimate of  $\xi_i$  can be made as follows. For a diffusing particle with diffusion constant  $D$  the velocity randomization time  $\tau$  is  $\sim 6D$ . This can be obtained from the following simple consideration. The average distance a particle with a velocity randomization time  $\tau$  diffuses in a given direction in time  $t$  is  $\langle z^2 \rangle = \frac{1}{3} t \tau$ . On the other hand the solution to diffusion equation  $\partial_t n = D \nabla^2 n$  with a point like source:  $n(\vec{r}, t) \sim \frac{1}{t^{3/2}} e^{-r^2/4Dt}$  specifies:  $\langle z^2 \rangle = \langle r^2 \rangle / 3 = 2Dt$ . A simple comparison of the two gives  $\tau \sim 6D$ . Using this decay time for a flux injected at velocity  $v_i$ , we estimate  $\xi \sim 6D_i v_i$ .  $\xi$  can also be taken to include other suppressions of the injected flux which may be relevant. We will return to a discussion of this question in section 8.

Finally we look for solutions which are stationary in the rest frame of the wall, i.e. of the form  $n(z, t) \equiv n(z - v_w t)$ . The equations are then

$$D_i n_i'' + v_w n_i' - \sum_A \Gamma_A (\sum_j k_j^A n_j) = \xi_i J_i^0 \delta'(z - v_w t) \quad (36)$$

where  $k_i^A$  is the factor which results when we express the decay terms in terms of the particle densities and  $\Gamma_A = \frac{12}{T^3} \bar{\Gamma}_A$ . The problem now becomes that of determining the baryon density behind the wall (in the broken phase where we take the electroweak sphaleron processes to be turned off) when a flux of some species is injected in front of the wall.

## 6. Solution of the Propagation Equations

To understand the solution of these equations let us first consider the case in which a chiral tau lepton flux is injected by the wall. The only decay processes we will consider are the Higgs mediated processes shown in Figure 3 and the electroweak sphaleron processes. In the unbroken phase there are no other processes which cause a chiral lepton to decay; in the broken phase there are other vev-suppressed processes but we will neglect these, taking them to be slow in a sense which will become more precise through our analysis. For the moment we will assume that the electroweak sphalerons are too slow to significantly alter the densities in front of the wall and thus that they too can be neglected, except for their role in making baryons. The Higgs processes bring about a coupling between the tau leptons and several other species ( Higgs particles, weak gauge bosons, quarks). For simplicity let us assume that these induced densities in species other than tau leptons can be neglected. We will later relax these assumptions and treat the full set of coupled equations. We then have

$$\begin{aligned} D_L L_L'' + v_w L_L' - \Gamma_{LR}(aL_L - bL_R) &= \xi_L J_0 \delta' \\ D_R L_R'' + v_w L_R' + \Gamma_{LR}(aL_L - bL_R) &= -\xi_R J_0 \delta' \end{aligned} \quad (37)$$

where we keep  $a = \frac{1}{2}$  and  $b = 1$  as variables for heuristic purposes. Left handed particles come as isospin doublets, but only one particle participates in each interaction. This explains  $k_L \equiv a = 1/2$ . The problem of solving (37) reduces to the corresponding homogeneous equations subject to the boundary conditions

$$\begin{aligned} D_L L_L|_{-}^{+} &= \xi_L J_0 & D_L L_L' + v_w L_L|_{-}^{+} &= 0 \\ D_R L_R|_{-}^{+} &= -\xi_R J_0 & D_R L_R' + v_w L_R|_{-}^{+} &= 0 \end{aligned} \quad (38)$$

which are derived by integrating up the equations through  $z = 0$ , imposing the conditions that the  $L_L$  and  $L_R$  are at most step-like discontinuous across the wall and that they are zero at  $+\infty$  (in the unbroken phase).

Substituting the ansatz  $e^{-\mu z}$  into (37) we find that the exponents are the roots of the equation

$$D_L D_R \mu^4 - v_w (D_L + D_R) \mu^3 + [v_w^2 - \Gamma_{LR}(aD_R + bD_L)] \mu^2 + v_w (a + b) \Gamma_{LR} \mu = 0. \quad (39)$$

This gives a constant solution and a cubic which has two real positive roots and one negative root. Requiring that the solutions be zero at  $+\infty$  and finite at  $-\infty$  we have eight constants to determine in the solutions:

$$\begin{aligned} L_L &= L_1 e^{-\mu_1 z} + L_2 e^{-\mu_2 z} & z > 0 \\ &= L_3 e^{-\mu_3 z} + L_4 & z < 0 \\ L_R &= R_1 e^{-\mu_1 z} + R_2 e^{-\mu_2 z} & z > 0 \\ &= R_3 e^{-\mu_3 z} + R_4 & z < 0 \end{aligned} \quad (40)$$

where  $\mu_3$  is negative. The conditions (38) fix only four of these constants. The additional condition required is found by adding the equations and integrating. This tells us that

$$D_L L'_L + D_R L'_R + v_w L_L + v_w L_R \quad (41)$$

is a constant of motion. By fixing it everywhere we can determine all the constants.

This conserved quantity (41) is simply the dynamical version of lepton number conservation which is built into the equations. More generally there is exactly one such relation for every quantity conserved by the decay processes we include in (36).  $B-L$  conservation, for example, will take the form

$$D_{q_L} B'_L + D_{b_R} B'_R + D_{t_R} T'_R - D_{l_L} L'_L - D_{l_R} L'_R + v_w (B - L) = 0 \quad (42)$$

where  $D_{q_L}$  is the diffusion constant for left-handed quarks etc. If all the diffusion constants are equal and the injected  $B-L$  is zero then  $B-L$  will be zero everywhere. However since in general the various species diffuse differently this will result in non-zero  $B-L$  locally, consistent with the constraint of global  $B-L$  conservation embodied in (42).

If we can solve the equations (37) to find  $L_L$  we can then use (6) to find the induced baryon number. Taking the baryons to be thermalized they appear as a flux  $-v_w B$  in the wall frame and therefore

$$\dot{B} = -v_w \partial_z B = -6N_F \frac{\bar{\Gamma}_s}{T^3} L_L \equiv -\Gamma_s L_L. \quad (43)$$

This equation is simply the limit of the appropriate diffusion/decay equation for baryon number which results when we use the fact that the diffusion constant of the quarks is very much less than the diffusion constants of the leptons, which source the equation. Integrating up  $L_L$  as in (40) we find the baryon number on the wall to be

$$B(0) = -\frac{\Gamma_s}{v_w} \left( \frac{L_1}{\mu_1} + \frac{L_2}{\mu_2} \right) \quad (44)$$

Thus we need simply to determine  $L_1$  and  $L_2$  by solving the cubic equation for the roots and the boundary problem.

We can solve (39) approximately in two different limits:

**Case 1.**  $v_w^2 \gg \Gamma_{LR}(aD_R + bD_L)$ .

In this limit the roots are

$$\mu_3 = -(a+b) \frac{\Gamma_{LR}}{v_w} \quad \mu_1 = \frac{v_w}{D_L} + \frac{a\Gamma_{LR}}{v_w} \quad \mu_2 = \frac{v_w}{D_R} + \frac{b\Gamma_{LR}}{v_w} \quad (45)$$

and, using the boundary conditions (38) and (41), we find

$$\begin{aligned} L_1 &= \frac{\xi_L}{D_L} J_0 & R_2 &= -\frac{\xi_R}{D_R} J_0 \\ L_2 &= \frac{b\Gamma_{LR} D_R}{v_w^2} R_2 & R_1 &= \frac{a\Gamma_{LR} D_L}{v_w^2} L_1. \end{aligned} \quad (46)$$

From (44) we then have

$$B(0) = -\left(\frac{\xi_L}{D_L} J_0\right) \left[ \frac{\Gamma_s D_L}{v_w^2} - \frac{\Gamma_s (b D_R + a D_L) \Gamma_{LR} D_R}{v_w^2} \right]. \quad (47)$$

We have taken  $\xi_L/D_L = \xi_R/D_R$ , assuming  $\xi_i \sim D_i$  from our estimate above. The first factor in (47) is the amplitude of the diffusing flux, down by  $\xi_L/D_L$  relative to the injected flux amplitude due to back diffusion across the wall. The expression inside the brackets is a conversion factor of this injected flux to baryons.

**Case 2.**  $v_w^2 \ll \Gamma_{LR}(aD_R + bD_L)$

Now the roots are

$$\mu_1 = \frac{a+b}{aD_R + bD_L} v_w \quad \mu_2 = -\mu_3 = \sqrt{\Gamma_{LR}(aD_L^{-1} + bD_R^{-1})} \quad (48)$$

and the solutions

$$\begin{aligned} L_1 &= \frac{b}{a} R_1 & R_1 &= -\frac{aD_R}{aD_R + bD_L} \left(\frac{\xi_R}{D_R} J_0\right) + \frac{aD_L}{aD_R + bD_L} \left(\frac{\xi_L}{D_L} J_0\right) \\ L_2 &= \frac{bD_R}{aD_R + bD_L} \left(\frac{\xi_R}{D_R} J_0\right) + \frac{aD_R}{aD_R + bD_L} \left(\frac{\xi_L}{D_L} J_0\right) & R_2 &= -\frac{D_L}{D_R} L_2 \end{aligned} \quad (49)$$

to leading order in both  $v_w^2/\Gamma_{LR}D_R$  and  $v_w^2/\Gamma_{LR}D_L$ . (48) and (49) give

$$B(0) = \left(\frac{\xi_L}{D_L} J_0\right) \frac{\Gamma_s (D_R - D_L)}{v_w^2} \frac{b}{a+b}. \quad (50)$$

These two limits of these equations have a simple explanation. The mean time a particle with diffusion constant  $D$  spends in the unbroken phase before it is captured by the wall is  $\sim D/v_w^2$ . If, as in case 1, this is long in comparison with the decay time  $\Gamma^{-1}$  then the solution describes the two injected fluxes diffusing with a perturbation to each of order  $\Gamma_{LR}D/v_w^2$  which tells us how the two species are sourced by one another through the decay process. Likewise since  $B$  violation has been assumed to be a slow process and there is no injected  $B$  the conversion factor is for the same reason  $\Gamma_s D/v_w^2$ . (47) therefore simply shows how  $B$  is sourced directly by the injected  $L_L$  and indirectly by the decay of the injected  $L_R$  into  $L_L$ . The precise coefficients can be read off from the decay term. We note that the signs of the contributions are opposite and therefore that there can be (for certain decay and diffusion constants) a critical wall velocity  $v_w$  for which they will precisely cancel.

The second case above is that in which the particles have time to decay before they are caught by the wall. In the  $\mu_1$  solution which extends furthest into the unbroken phase the left and right-handed leptons are in abundances such that the decay process is approximately (to corrections of order  $v_w^2/\Gamma_{LR}D$ ) in equilibrium i.e.  $L_1 = \frac{b}{a} R_1$ . Working to leading order in  $D_L/D_R \ll 1$  we have  $R_1 = -\frac{\xi_R}{D_R} J_0$ . The right-handed lepton density is simply equal to the effective injected flux and then putting the decay process in equilibrium determines the density of left-handed leptons. We can also read off  $\mu_1$  from the

lepton number conservation constraint (41), since each exponential solution individually will satisfy this, by simply putting in the equilibrium constraint. The profile of left-handed leptons which act as a source in the baryon number violation equation (43) is

$$-\frac{b}{a}\left(\frac{\xi_R}{D_R}J_0\right)e^{-\frac{a+b}{a}\frac{v_w}{D_R}z}. \quad (51)$$

We note that this is different from what one would infer if one took the local densities to be determined by the equilibrium constraint and a lepton density taken to be carried by the right-handed leptons diffusing in front of the wall. This calculation gives the profile

$$-\frac{b}{a+b}\left(\frac{\xi_R}{D_R}J_0\right)e^{-\frac{v_w}{D_R}z}. \quad (52)$$

which, however, when integrated gives the same baryon number  $B(0)$ .

We can in fact generalize the simple argument used to determine this sort of ‘long tail’ solution when there are  $n$  coupled equations, with one species which diffuses more efficiently than any other. Firstly we enforce the equilibrium constraints on all the appropriate decay processes. The equations then have  $n - A$  conservation laws of the form of (41) and (42), where  $A$  is the number of decay processes in equilibrium. We can write all but one of these as linear combinations excluding the species which diffuses in the long tail solution. It follows from the conservation laws that these linear combinations can be set equal to zero to leading order in the ratio of the diffusion constant of any other species to the one diffusing in the long tail. We now can determine all amplitudes in the solution in terms of the amplitude of the diffusing quantity. By substituting these back in the final conservation law involving this species we can then determine  $\mu_1$  for the solution. Finally we need to convince ourselves that the amplitude in this exponential solution really is equal (to leading order) to the effective injected flux for that species. To see this one writes down the boundary condition giving the jump in the density at the wall for the species which diffuses in the long tail e.g.

$$D_R(R_1 + R_2 + R_3 + \dots) = \xi_R J_0. \quad (53)$$

Using the same conservation law applied to all the other solutions individually one can see that the amplitudes of all of them ( $R_2, R_3$  etc.) are next to leading order relative to the amplitude of the long tail  $R_1$ , provided the amplitude of the source for all other species is not larger than that for the diffusing species.

Let us now summarize this procedure which we will use to extract the information we need to calculate the baryon asymmetry from the full set of decay equations :

- 1. Identify how the injected fluxes of species with diffusion constants  $D_i$  can source left-handed fermion number significantly for the relevant wall velocity  $v_w$ . Either they do so directly or through some decay process with rate  $\Gamma$  which satisfies  $\frac{D_i\Gamma}{v_w^2} > 1$ .

- 2. Consider only the single species with the *longest* diffusion length  $D_o$  which is injected (flux  $J_o$ ) and sources left-handed fermion number. The amplitudes we need to determine are those in a solution  $n_i(z) = n_i(0)e^{-\mu z}$  which describes the diffusion of this species and its sourcing of other species through decay processes ( $\mu \sim v_w/D_o$ ).

•3. Identify all the  $A$  decay processes which satisfy  $\frac{D_o\Gamma}{v_w^2} > 1$ . Impose the condition that the appropriate signed sum of the particle density amplitudes (assumed linearly proportional to the chemical potentials) corresponding to each process is equal to zero.

•4. Identify the remaining  $n - A$  linear combinations of particle densities conserved by the  $A$  equilibrated processes in step 3, and write them so that the density of the sourcing species appears in only one linear combination. Set all but this latter linear combination to zero and so determine the amplitude of all species  $n_i(0)$  in terms of the sourcing species amplitude, which is just  $\frac{\xi_o}{D_o} J_o$  ( $\xi_o$  the appropriate persistence length).

•5. To determine the root  $\mu$  of the exponential decay tail corresponding to the solution use the remaining conserved linear combination in the form (42) with all diffusion constants but  $D_o$  set equal to zero, and all the amplitudes in the coefficient of  $v_w$  solved in terms of the sourcing species amplitude from step 4.

•6. If the baryon number violating processes were amongst the equilibrated processes in step 3 the final baryon asymmetry is simply the amplitude of the baryon number in the solutions just determined. If the baryon number violating processes are not equilibrated, the solution for the total left-handed fermion number must be used as a source in  $\dot{B} = -\Gamma_s(3B_L + L_L)$  which simply gives  $B(0) = -\frac{\Gamma_s}{v_w\mu}(3B_L + L_L)(0)$ .

For our analysis of the case of injected leptons this will be adequate to determine the baryon number in all the different cases of interest. For top quarks the solution of these equations is complicated by the fact that the leading contribution from these ‘long tail’ solutions vanishes in various cases so that the steps following the second above are not applicable. We will then have to extend our analysis to find the contributions from other solutions which we will have to determine more carefully. However, as we will discuss below, we will limit ourselves in this case to a qualitative analysis of the resulting asymmetry.

### 6.1 Baryon Asymmetry from an Injected Tau Lepton Flux

We now consider in detail the baryon asymmetry produced in various regimes by an injected flux in tau leptons. First we note the numerical values of the parameters which we need. In Appendix C we calculate the diffusion constants taking into account the dominant  $t$  channel gauge boson exchange diagrams in Figure 5

The results are

$$\begin{aligned} D_L^{-1} &= 8\alpha_W^2(1 + 0.8 \tan^4 \theta_w)T \approx \frac{T}{100} \\ D_R^{-1} &= 28\alpha_W^2 \tan^4 \theta_w T \approx \frac{T}{380} \\ D_q^{-1} &= 8\alpha_s^2 T \approx \frac{T}{6} \end{aligned} \tag{54}$$

where  $\theta_W$  is the Weinberg angle [35]. Note that the right-handed leptons which are coupled only through hypercharge interactions have a very long diffusion length:  $D_R \approx 380/T \approx 4D_L$ .

In Appendix D we calculate the rates in a plasma for the perturbative decay processes mediated by Higgs bosons as in Figures 3. For these we find

$$\Gamma_q = 0.2\alpha_s y_t^2 \quad \Gamma_{LR} \equiv \Gamma_{\tau_R} = 2\Gamma_{\tau_L} = 0.3\alpha_w y_\tau^2 \tag{55}$$

where  $y_t$  and  $y_\tau$  are the Yukawa couplings for the top quark and tau lepton respectively. The rates for the Higgs exchange process in Figure 4 is also calculated in Appendix D,

but we will not make use of it as it is subdominant for the cases of interest to us. The normalizations of these rates are defined by the convention in (36). Note that this means we do not incorporate the counting factor (for color and isospin) into the rate, just as in the case we have discussed where  $\Gamma_{LR}$  was defined so that a factor of  $1/2$  appeared in front  $L_L$  because of the two isospin states.  $\Gamma_A$  in (36) is just the collision rate per unit volume, divided by a factor  $T^3/12$ .

For the anomalous processes we have  $\nu_i$  in (36) differing from unity and the convention we have adopted is an awkward one. Instead we define the rates as the coefficients in

$$\dot{B} = -\Gamma_s(3B_L + L_L) \quad \dot{\Delta} = -\Gamma_{ss}\Delta \quad (56)$$

where  $\Delta = B_L - B_R$ . The second equation is derived by the same arguments outlined in section 2. These give

$$\Gamma_s = 6N_F\kappa_s\alpha_W^4 T \approx 2 \times 10^{-5}\kappa_s T \quad \Gamma_{ss} = 64\kappa_{ss}\alpha_S^4 T \approx \kappa_{ss} \frac{T}{40}. \quad (57)$$

where we have adopted the standard conventions in which  $\kappa_s\alpha_W^4 T^4$  and  $\frac{8}{3}\kappa_{ss}\alpha_W^4 T^4$  are the number of topology changing processes per unit volume per unit time, and  $N_F = 3$  is the number of families.

Numerical simulations give values of  $\kappa_s$  and  $\kappa_{ss}$  in the range  $0.1 - 1$  [36]

**Case 1:**  $v_w^2 > \Gamma_\tau D_R, \Gamma_s D_R$ .

This is simply case 1 as treated above with  $B(0)$  as in (47). The Higgs processes do not have time to equilibrate the injected particles with any other species, and the baryons are produced directly from the injected left-handed leptons and from the fraction of the injected right-handed leptons converted to left-handed leptons.

**Case 2:**  $\Gamma_\tau D_R > v_w^2 > \Gamma_s D_R$ .

Now the  $\Gamma_\tau$  processes can equilibrate in the right-handed lepton diffusion tail. This creates a source for Higgs particles which couple in turn to quarks. We work for definiteness in a model in which one Higgs doublet  $\phi_1$  is coupled to the charge  $\frac{2}{3}$  quarks and the second doublet  $\phi_2$  to the charge  $-\frac{1}{3}$  quarks and leptons. We take all the processes in Figures 3 and 4 to be in equilibrium as well as the strong sphaleron. Other permutations and possible Higgs couplings can also be considered in a way which will be clear from this example. Following the general procedure outlined above we must therefore impose

$$\begin{aligned} \frac{1}{2}\tau_L - \tau_R - \frac{1}{4}\phi_2 &= 0 & \text{for } \tau/\text{Higgs} \\ \frac{1}{6}q_L - \frac{1}{3}b_R - \frac{1}{4}\phi_2 &= 0 & \text{for bottom/Higgs} \\ \frac{1}{6}q_L - \frac{1}{3}t_R - \frac{1}{4}\phi_1 &= 0 & \text{for top/Higgs} \\ q_L + n_L - t_R - b_R - n_R &= 0 & \text{for strong sphalerons} \end{aligned} \quad (58)$$

where  $\tau_L$  is the density of left-handed tau leptons and tau neutrinos (minus their anti-particles),  $\phi_1$  the density of Higgs particles of both charges in doublet  $\phi_1$ ,  $q_L$  the density

of left-handed tops and bottoms,  $n_L$  the density of left-handed quarks in the lighter two generations, etc. The numerical factors are the counting factors for color and isospin, and also a factor of 2 for fermions relative to bosons which enters in the conversion from chemical potential to number density. The gauge bosons cancel out because when we subtract the equilibrium constraints for the processes involving all the anti-particles from those for the processes involving the particles. The conservation relations which we use to solve for all densities in terms of  $\tau_R$  are

$$\begin{aligned}
q_L + t_R + b_R &= 0 \\
\tau_L + \phi_2 - b_R - \frac{1}{4}n_L &= 0 \\
\phi_1 - t_R - \frac{1}{4}n_L &= 0 \\
n_L + n_R &= 0.
\end{aligned}
\tag{59}$$

We find these by simply determining directly the linear combinations conserved by the processes which we have put in equilibrium. Together (58) and (59) give  $3B_L + L_L = q_L + n_L + \tau_L = \tau_L = \frac{182}{118}\tau_R$ , and following the procedure outlined above we calculate that in the ‘long tail’ solution the profile of  $3B_L + L_L$  is

$$-\frac{182}{118} \left( \frac{\xi_R}{D_R} J_0 \right) e^{-\frac{300}{118} \frac{v_w}{D_R} z}.
\tag{60}$$

which integrates to give

$$B(0) = \frac{182}{300} \frac{\Gamma_s D_R}{v_w^2} \left( \frac{\xi_R}{D_R} J_0 \right).
\tag{61}$$

We note that the correction obtained over a calculation neglecting all species except the tau leptons is negligible: the factor  $\frac{182}{300}$  replaces  $\frac{2}{3}$ , which follows from  $\tau_L = 2\tau_R$  and  $\mu_1 = 3v_w D_R^{-1}$ .

**Case 3:**  $\Gamma_\tau D_R, \Gamma_s D_R > v_w^2 > \Gamma_s D_L$

In this case the sphalerons have time to reach equilibrium in the  $D_R$  tail. We must now simply add the constraint

$$q_L + n_L + \tau_L + l_L = 0
\tag{62}$$

where  $l_L$  are the left-handed leptons in the two lighter generations. We also revise the conservations laws (59) by adding  $l_L$  with the appropriate coefficient to each of them so that they also invariant in electroweak sphaleron processes. We then proceed as before and calculate the equilibrium density of  $B$  at the wall (which is just the amplitude of the solution) to be

$$B(0) = -\frac{210}{307} \tau_R(0) = \frac{210}{307} \left( \frac{\xi_R}{D_R} J_0 \right).
\tag{63}$$

Neglecting all species but the tau leptons we would solve  $3B_L + \tau_L = 0$ ,  $B_L = B_R$  and  $\tau_L = 2\tau_R$  to get  $B(0) = \frac{4}{3} \left( \frac{\xi_R}{D_R} J_0 \right)$ , which differs by a factor of two from what we have calculated including all species.



**Case 4:**  $\Gamma_s D_L > v_w^2 > \Gamma_\tau D_R$ .

Here the tau lepton-Higgs processes are too slow to allow the right-handed particles act as a source for baryon number, but the left-handed leptons are diffusing long enough to allow the baryon number violating processes reach equilibrium. Since these couple the leptons to the quarks we must impose all the constraints in (58) above except the first one. We use the same conservation laws as in case 3, simply removing  $\tau_L$  in the appropriate way from the second one. Solving for  $B(0)$  we find

$$B(0) = -\frac{6}{13}\tau_L(0) = -\frac{6}{13}\left(\frac{\xi_L}{D_L}J_0\right). \quad (64)$$

which again is a very minor alteration of the naive result  $B(0) = -\frac{2}{3}\tau_L(0)$ , which follows from imposing  $B_L = B_R$  and  $3B_L + \tau_L = 0$ .

## 6.2 Baryon Asymmetry from an Injected Top Quark Flux

We will not treat the case of an injected top quark flux in great detail. Unless the walls are very thin they are likely to be very poorly described by our analytic calculation because (i) we require  $L_w \ll m.f.p$ , and (ii) we calculated all our expressions in the case that  $m_f < m_H$ , which means for the top quark  $L_w \sim m_H^{-1} < m_t^{-1} \sim 2/T$ . We will discuss these criteria in further detail in section 8.

In the accompanying paper [26] we develop a new formalism for the treatment of quarks when scattering is taken into account. The case of top quarks in the thin wall regime has also been studied by CKN in their original exposition of the ‘charge transport’ mechanism in [21], and our main interest here has been to explore the interesting possibility that leptons might source this sort of baryogenesis. For the purposes of comparison with these previous calculations and with our calculations in [26] however it is of interest to turn to this case with the insight we have gained by studying the case of leptons. The analysis we sketch can be carried through rigorously and leads to the results which we give below.

CKN calculated the baryon asymmetry by considering the injection of a hypercharge flux into the unbroken phase. The diffusion of this flux was modeled numerically and the resulting profile used as a source for a local thermal equilibrium calculation, in which the various conserved global charges were set to zero. In [24] we pointed out that these constraints are not strictly appropriate as the local densities of global charges may float, *i.e.* are not necessarily confined to their globally constrained values. In the case of leptons we have just treated this is very clear e.g.  $B - L$  becomes locally non-zero despite the fact that it is zero in the injected flux. The method we have developed above allows us to treat this dynamical determination of the global charges and it is interesting to ask what effect this has in the case of quarks. A second correction to the calculation of CKN is that which is required because of strong sphalerons. It was pointed out in [27] that CKN’s local thermal equilibrium calculation gives a null result when these processes are put in equilibrium. The method we have developed allows us to see the effect of a finite strong sphaleron rate and calculate the correction it leads to.

We will assume again that we have a model in which one doublet is coupled to the charge  $\frac{2}{3}$  quarks and the other to the charge  $-\frac{1}{3}$  quarks and leptons. We will take the Yukawa couplings for the latter to be small so that the only Higgs coupling which is relevant over the time in which particles are diffusing is the top quark one.

The simplest case we can treat is when  $v_w^2 > \Gamma D_q$  for all decay processes. Then the injected left-handed baryon number drives  $B$  violation directly, and is caught before there is any significant coupling to any other species. We read off

$$B(0) = -\frac{3\Gamma_s D_q}{v_w^2} \left( \frac{\xi}{D_q} J_0 \right). \quad (65)$$

where  $\xi$  is as before the persistence length of the injected current.

However from (54), (55) and (57) we see that the equilibrium condition  $v_w^2 < \Gamma D_q$  is actually satisfied for typical non-relativistic velocities  $v_w \sim 0.1$  for both the top/Higgs processes ( $v_w^2 < \frac{y_t^2}{8}$ ) and the strong sphalerons ( $v_w^2 < \frac{\kappa_{ss}}{9}$ ). We cannot proceed however precisely as we did in the analysis of an injected lepton flux for two reasons:

- If we take the left and right-handed quarks to have the same diffusion constant the conservation law (in the absence of weak sphalerons)

$$D_q B' + v_w B = 0 \quad (66)$$

for baryon density  $B$  forces  $B = 0$  everywhere. In the ‘long tail’ solution in which we impose the equilibrium constraints on the strong sphalerons we have  $B_L = B_R$  and therefore, as explained in section 2, since  $B_L = L_L = 0$ , there is no force driving  $B$  violation.

- Our analysis relied on the assumption that the sourced species which diffuses furthest is directly sourced by the injected current. This is not true now because the Higgs particles which are sourced indirectly by the decay processes have a diffusion constant  $D_\phi \sim D_L$  (for the left-handed lepton), much larger than that of the directly sourced quarks.

To disentangle the implications of these two points we first neglect the Higgs processes completely. The first point is true irrespective of whether the Higgs processes are turned on or not, and when we have clarified its implications we will return to this second point. We consider then the equations for the left and right-handed baryons to which our diffusion equations reduce in the absence of the Higgs processes:

$$\begin{aligned} D_{q_L} B_L'' + v_w B_L' - \frac{\Gamma_{ss}}{2} (B_L - B_R) - 3\Gamma_s B_L &= \xi_L J_0 \delta' \\ D_{q_R} B_R'' + v_w B_R' + \frac{\Gamma_{ss}}{2} (B_L - B_R) &= \xi_R J_0 \delta' \end{aligned} \quad (67)$$

where  $D_{q_L}$  and  $D_{q_R}$  are the diffusion constants for left- and right-handed quarks respectively. We consider these equations in two cases:

**Case 1:**  $D_{q_L} = D_{q_R} = D_q$ . We add and subtract the two equations (67) to get two equations for  $B$  and  $\Delta = B_L - B_R$

$$\begin{aligned} D_q B'' + v_w B' - \frac{3\Gamma_s}{2} (B + \Delta) &= 0 \\ D_q \Delta'' + v_w \Delta' - \frac{3\Gamma_s}{2} (B + \Delta) - \Gamma_{ss}(\Delta) &= 2\xi J_0 \delta'. \end{aligned} \quad (68)$$

The  $\Gamma_s$  term can be neglected in the second equation, and the solution for  $\Delta$  obtained is  $\frac{\xi}{D_q} J_0 \exp -\sqrt{\Gamma_{ss}/D_q} z$  to leading order in  $v_w/\sqrt{\Gamma_s D_q}$ . This is then used as a source term in the first equation for  $B$ , and the resulting baryon asymmetry at the wall is

$$B(0) = -\frac{1}{2} \frac{v_w}{\sqrt{\Gamma_{ss} D_q}} \frac{3\Gamma_s D_q}{v_w^2} \left( \frac{\xi}{D_q} J_0 \right). \quad (69)$$

We see that the effect of including the strong sphalerons is to produce a suppression by the factor  $v_w/2\sqrt{\Gamma_{ss} D_q} \approx v_w/.7\sqrt{\kappa_{ss}}$  of the result in (65).

The factor of  $\frac{1}{2}$  can be simply understood. It arises when we solve the second equation in (68). The boundary conditions impose a jump across the wall of  $\xi/D$ . When  $v_w^2 > \Gamma_{ss} D_q$  the amplitude in front of the wall is  $\approx \xi/D$  and the amplitude behind suppressed. When  $v_w^2 < \Gamma_{ss} D_q$  the amplitude of the solution behind is equal and opposite to that in front, and the roots equal, so that exactly half the injected flux appears in front of the wall, and half behind. The explanation for this behavior is simply that in the low velocity limit the decays play the role of dissipating the injected asymmetry so that the motion of the wall becomes unimportant and the solution approaches the symmetrical one. In the other limit the injected flux is dissipated by the wall catching up with the diffusing particles and the only stationary solution is reached by particles piling up in front of the wall so that the back diffusion current exactly cancels the injected current.

**Case 2:**  $D_{qR} - D_{qL} = \delta D \neq 0$ .

In this case the argument that there is no contribution from the long tail breaks down because  $B$  is not zero locally in front of the wall. To treat this case we consider the altered version of (68), in which there is now a source for  $B$ , look for the contribution from a solution with  $\Delta = 0$ . The equation for  $B$  can be shown to be

$$\overline{D}_q B'' + v_w B' - \frac{3\Gamma_s}{2} B = -\frac{\delta D}{D_q} \xi J_0 \delta' \quad (70)$$

where we have taken  $\xi \propto D$  for the two chiralities. The solution for the baryon density behind the wall is

$$B(0) = \frac{1}{2} \frac{\delta D}{\overline{D}_q} \frac{3\overline{\Gamma}_s D_q}{v_w^2} \left( \frac{\xi}{D_q} J_0 \right). \quad (71)$$

$\overline{D}_q \approx 1/12\alpha_s^2 T$  is the average of the two diffusion constants.

If we take  $\delta D$  to arise from the difference in left and right-handed quark diffusion because of  $SU(2)$  processes like those in Figure 5, we use our calculations for the case of leptons to estimate  $\frac{\delta D}{D_q} \approx (\alpha_W/\alpha_s)^2 \approx 1/20$ . A difference in the diffusion constants also results when one incorporates the Higgs processes in Figure 3, for which the scattering rates differ by a factor of two for the quarks of different handedness. A naive estimate from our calculated rates (55) indicates that this would give  $\delta D$  of the same order. So for low wall velocities and/or large  $\kappa_{ss}$  (71) indicates that the dominant effect can still come from the diffusion tail. The suppression due to the strong sphalerons in (69) is cut off when one takes into account the slightly different transport properties of the left- and right-handed baryons.

Finally we return to the second difference we noted between the case of quarks and that of the leptons - that the particle species which diffuses furthest are the Higgs particles which we have assumed not to be directly sourced by reflection from the wall. Including the Higgs processes should not alter significantly the solutions we have just considered. As in the case of the leptons these processes will simply cause a redistribution of the injected asymmetries between the species coupled through these processes, and this will lead simply to minor numerical corrections. The important point is that these processes do not drive the quantity driving baryon number to zero as the strong sphalerons do. In neglecting the Higgs processes, however, we did overlook the new ‘long-tail’ solutions for the Higgs particles which are sourced indirectly through the decay processes. Can these particles which diffuse much further than the quarks themselves in turn source significant baryogenesis? By examining the boundary conditions in the way we did in the lepton case (choosing this time to write down a conservation law involving  $\phi$  and a combination of quarks which is sourced) one can show that the amplitude of this solution is down by approximately  $D_q/D_\phi$ , relative to the directly injected diffusion tail. When integrated therefore, we expect, the two solutions should give the same order contribution. However the further suppression due to strong sphalerons which we have just discussed will be greater (by  $\sim \sqrt{D_q/D_\phi}$ ) for the longer tail since the baryons are diffusing longer, and therefore we anticipate that no significant additional baryogenesis will occur because of the efficient diffusion of Higgs particles. This qualitative analysis can be carried through rigorously just as in the lepton case by fully solving the diffusion/decay equations with the appropriate boundary conditions.

## 7. Screening

In the treatment of the problem we have presented we have so far entirely neglected the effect of hypercharge screening. The original mechanism of this sort proposed by CKN described the problem in terms of a hypercharge flux generated by the reflection of top quarks off the wall. It was pointed out by Khlebnikov [37] that this treatment overlooked the fact that any such hypercharge density would in fact be very efficiently screened by the plasma. Since it is hypercharge that was described as driving the production of the asymmetry it appeared that this will cause a very significant attenuation of the effect. This criticism applies to the mechanism as we have treated it as well. If one computes the hypercharge density profile in front wall in any of the stationary solutions to our diffusion equations the result is non-zero. CKN in a later paper [38] argued that the effect of screening could be accounted for by doing their constraint calculation with injected  $Y$  in a different basis of charges ‘orthogonal’ to  $Y$ . One of the charges named  $X$  which is a linear combination of hypercharge and baryon number is identified as the appropriate injected charge which drives the  $B$  violation. Here we will attempt to clarify this question of the role of hypercharge screening, justifying the approximation we have made in neglecting it and outlining how it can be incorporated in these calculations.

Consider first a system in a constrained thermal equilibrium, with chemical potentials  $\mu_i$  for species  $i$ . Suppose now we apply a local potential for hypercharge  $\phi_Y(x)$  in some region. The local thermal equilibrium with the same chemical potentials is

$$f_i(p, x) = \frac{1}{e^{\beta(\epsilon_i + y_i \phi_Y(x) - \mu_i)} \pm 1} \quad \text{where} \quad \epsilon_i = \sqrt{p^2 + m_i^2}. \quad (72)$$

This makes the collision integral on the right hand side of the Boltzmann equation zero if the original chemical potentials  $\mu_i$  did. This is true because shifting the chemical potential by an amount  $y_i\phi_Y(x)$  does not alter the rates of processes which conserve hypercharge. This distribution function describes a solution in which the potential has the effect of drawing in an amount of each species proportional to its hypercharge, but this is the only change admitted to the local density of any species. It is this local equilibrium which CKN calculated in [38], fixing the potential  $\phi_Y(x)$  by requiring it to screen the hypercharge density in (72) to zero. The same  $\mu_i$  as in the unscreened case are obtained by their prescription of working with ‘orthogonal’ charges. These are simply the linear combinations of charges which are unchanged by screening i.e. charges  $Q_A = \sum_i q_A^i n_i$  in which  $\phi_Y(x)$  cancels out because  $Tr(QY) \equiv \sum_i k_i q_A^i y_i = 0$ , where  $k_i$  is a statistical factor which is one for fermions and two for bosons in the massless approximation. Imposing the same constraints given by a calculated injected flux on these charges amounts to solving precisely the same set of linear equations as in the unscreened case, except for the one setting the hypercharge to zero. Quite simply one is taking the previous solution and superimposing on it the extra screening densities which leave rates unchanged. In particular one finds that the sphaleron rate is unchanged and hence the resulting asymmetry.

Is this a good approximation to the real process of screening? It describes correctly a static situation where some real physical constraint — an injected decaying flux or a force like that we describe in [26] — imposes the constraints on the  $\mu_i$  in some fixed region. Then this static equilibrium (72) satisfies the Boltzmann equation. However the cases we are considering are not manifestly like this. The region in which there are perturbations induced (described by locally varying chemical potentials  $\mu_i$ ) is moving and the screening is *dynamical*. The screening currents respond to the injected currents and the time it takes for them to screen the charges is important. In particular the static approximation breaks down because the response of different species to the driving hypercharge field is different because they have very different transport properties. To see this suppose a single species is injected by reflection from the wall. This injected flux carries positive hypercharge one way and compensating hypercharge the other way, which induces hypercharge currents in the other species across the wall. If all these other species are very “stiff” in comparison to the original species i.e. have much smaller diffusion constants, the screening will impede the diffusion we have described. However, if there are species with comparable transport properties (as there are in the electroweak plasma), the injected flux can be screened by these species and the effect should be simply that the injected flux drags along screening charges with it, with its behaviour little altered from that we have described. This is the picture which we will now briefly support with some simple quantitative arguments.

The way to include this dynamics is simply to incorporate screening in our calculations. We do this by adding the number current induced by the hypercharge field to the diffusion current using Ohm’s Law so that we have

$$\vec{J} = \vec{J}_d + \vec{J}_s = -D\vec{\nabla}n + \sigma\vec{E} \quad (73)$$

where  $\vec{E}$  is the hypercharge field induced by the local densities and  $\sigma$  is the conductivity. Note that this definition of conductivity differs from the usual one by a hypercharge factor  $y$ , because it relates the number current rather than the charge current to the field. The

conductivity may be related to the diffusion constant using the derivation of the diffusion constant given in Appendix C (see also [24]). The one difference is that the space varying chemical potential is replaced by the hypercharge potential. One arrives at a relation between the induced number current and the electric field which is exactly the same except as that between the diffusion current and the gradient in the chemical potential, with

$$\sigma = \frac{T^2}{6} y D \tag{74}$$

Incorporating this extra term in the derivation of the diffusion/decay equations (36) simply results, after using Gauss' law, in an extra term  $-4\pi\sigma_i Y$  in each equation. So we have a set of equations exactly like those we analyzed except for this extra coupling between all the species, which greatly complicates the analysis we presented.

In the limit in which all diffusion constants are equal, a general analysis is possible. Taking linear combinations we can rewrite the  $N$  equations (for  $N$  species) as  $N - 1$  equations in which the screening term cancels out, and one equation for the total hypercharge  $Y$  in which the decay terms cancel out (because total hypercharge is conserved). This corresponds precisely to going to the ‘orthogonal’ basis described by CKN. In this case then the only alteration to our equations is to add the screening term  $-4\pi\sum_i y_i \sigma_i Y$  (where the sum is over species) to the hypercharge propagation equation. This term is formally just like another decay process term and we can follow the sort of analysis given in section 6. The “equilibrium” condition (now for  $Y = 0$ ) becomes  $(v_w^2/4\pi\sum_i \sigma_i D) \ll 1$ . Thus for  $v_w < \sqrt{\frac{2\pi}{3}} \bar{y} D T$  (where  $\bar{y}^2 = \sum_i y_i^2$ ) the screening will be effective in the ‘long-tail’ diffusion solution, and in this regime we approach the static limit discussed by CKN. The new set of constraints on our ‘long-tail’ solution will be satisfied by superimposing a density of each species in proportion to its hypercharge on our previous solution. Note also that any ‘short-tail’ solution in which  $Y \neq 0$  will be restricted to a distance  $(\sqrt{\frac{2\pi}{3}} \bar{y} T)^{-1}$  of the wall, which is simply the inverse Debye mass in this model.

The diffusion constants of different particles in the electroweak plasma are however, as we have seen, very different, varying over two orders of magnitude. The current induced in response to a hypercharge field is therefore not proportional simply to the hypercharge of the responding species. The question which interests us is which particle species screen a given injected species and whether this can have any very significant effects on the solutions we analysed. In particular we would like to see the effect of the very different transport properties of the quarks and leptons in the screening of injected fluxes of either. We will not carry out a general analysis of the equations but limit ourselves to a simplified set of equations to illustrate the intuitive argument given above. The most important point is that the “stiffness” of quarks will not prevent the diffusion of leptons, because there are other leptons around which will screen the injected flux. Rather than drawing along quantities of each species in proportion to their hypercharge, the leptons will be screened by other leptons, not by quarks.

So consider the following simple model:

$$\begin{aligned}
D_A A'' + v_w A' - 4\pi\sigma_A(y_A A + y_B B + y_C C) &= s_A \delta' \\
D_B B'' + v_w B' - 4\pi\sigma_B(y_A A + y_B B + y_C C) &= 0 \\
D_C C'' + v_w C' - 4\pi\sigma_C(y_A A + y_B B + y_C C) &= 0.
\end{aligned} \tag{75}$$

The species  $A$  is sourced, while the species  $B$  and  $C$  screen. We have not included a decay term as this should not be important because all such decays are hypercharge conserving. Let us now study the roots of these equations and compare them to the unscreened analogue in which  $A$  simply diffuses as described by its own diffusion constant (i.e. in the solution with root  $v_w/D_A$ ).

To obtain an equation for the root of the screened solution we combine (75) to get two equations without the screening term which can be integrated once to give two first order equations. Requiring  $e^{-\lambda_D z}$  to be a solution and imposing  $Y = 0$  gives

$$\begin{aligned}
&D_A D_B D_C \left( \sum_I y_I^2 \right) \lambda_D^2 \\
&- v_w \left[ y_A^2 D_A (D_B + D_C) + y_B^2 D_B (D_C + D_A) + y_C^2 D_C (D_A + D_B) \right] \lambda_D \\
&+ v_w^2 \left[ D_A y_A^2 + D_B y_B^2 + D_C y_C^2 \right] = 0
\end{aligned} \tag{76}$$

Solving this equation in the limit  $D_C \ll D_A, D_B$  we find a ‘short’ root involving  $D_C$  and a ‘long’ root

$$\lambda_L = v_w \frac{D_A y_A^2 + D_B y_B^2}{D_A D_B (y_A^2 + y_B^2)} \rightarrow \begin{cases} \frac{v_w}{D} & \text{for } D_A = D_B = D \\ \frac{v_w}{D_B} \frac{y_A^2}{y_A^2 + y_B^2} & \text{for } D_A \gg D_B \end{cases} \tag{77}$$

We see that if there is one species  $C$  which has a very small diffusion constant, this does not shorten the previous solution provided there is a second species  $B$  available to screen which has comparable (or better) diffusion properties.

For baryogenesis we will typically want to evaluate the integral under the diffusion tail  $\int A$ . In this case, to leading order in  $D_C/D$ , species  $C$  does not screen in the long tail. Using this and the fact that the main contribution comes from the longer tail, one obtains  $\int A = \frac{s_A}{v_w} \frac{y_B^2}{y_A^2 + y_B^2}$ . The suppression with respect to the unscreened case for which  $\int A = \frac{s_A}{v_w}$  is due to the screening with species  $B$ . The second limit in (77) shows that the diffusion solution for  $A$  does not survive if both species have much shorter diffusion lengths — the solution is forced to follow the behaviour of the least ‘stiff’ of the screening species.

We now solve (76) in the limit  $D_A \sim D_B \ll D_C$ . We assume  $D_A = D_B = D$  which considerably simplifies potentially cumbersome algebra but still models the relevant effects of screening. This case is more complicated because there are two comparable roots

$$\lambda_S = \frac{v_w}{D} \qquad \lambda_L = \frac{v_w}{D} \frac{y_C^2}{\sum_I y_I^2} \tag{78}$$

A careful analysis using the appropriate boundary conditions and imposing the condition of zero total hypercharge with the ansatz  $I = I_S \exp[-\lambda_S z] + I_L \exp[-\lambda_L z]$  for  $z > 0$  and  $I = 0$  for  $z < 0$  (where  $I = A, B, C$ ) permits us to evaluate the amplitudes. We find that in the shorter tail ( $\lambda_S$ ) only species  $B$  screens;  $C$  does not screen at all (i.e. its amplitude is suppressed by  $D/D_C$ ). In the longer tail ( $\lambda_L$ ) something rather unexpected happens: species  $B$  anti-screens and  $C$  screens such that  $y_B B/y_C C = -y_B^2/(y_A^2 + y_B^2)$ . To answer how screening affects baryogenesis we again as above study  $\int A$ . Of course, if species  $B$  and  $C$  carry left handed fermion number, the final baryon asymmetry should include terms proportional to  $\int B$  and  $\int C$ , but let us ignore this complication. Recall that if one species ( $B$ ) screens with  $D_A = D_B = D$  we have  $\int A = \frac{s_A}{v_w} (y_B^2/y_A^2 + y_B^2)$ . When one adds a second species ( $C$ ) to screen with  $D_C \gg D$  one finds that the same result  $\int A$  for the contribution of the shorter tail (in which  $C = 0$ ). But the total result including the longer tail contribution is just  $\int A = s_A/v_w$  so that the unscreened result is recovered.

In the electroweak plasma there are many species to screen, in particular there are lighter families which have almost identical diffusion properties to the third family fermions. For example, in the case of baryogenesis sourced by the right-handed lepton diffusion described in section 6, we expect that the screening will be provided by all three families of leptons (mainly by the antiparticles of the right-handed leptons). Still however it will be only the  $\tau_R$  leptons which are converted to the left-handed leptons which source baryogenesis and we thus estimate in the spirit of the simple model above that the net result would be an attenuation by a factor of  $\frac{2}{3}$ . The second case studied above tells us that something rather nice occurs in the top quark mediated baryogenesis. The screening with other quarks alone has the tendency to decrease somewhat the baryon asymmetry. However the presence of mobile leptons and Higgs particles works in the direction of recovering the unscreened result. We conclude that the corrections due to screening of the results we calculated in section 6 should be numerical changes of order unity <sup>†</sup>.

## 8. Baryon to Entropy Ratio and Validity of Calculations

We now calculate the baryon asymmetry in its standard form before comparing the various cases we have considered. Assuming the asymmetry at the wall to be frozen in as it passes behind the wall i.e. that the weak sphaleron is switched off just behind the wall, we need simply divide  $B(0)$  by the entropy density  $s = \frac{2\pi^2}{45} g_* T^3$  ( $g_* \approx 100$  the number of relativistic degrees of freedom) to get the standard baryon number to entropy ratio. Using the flux in (25) we find, for the most interesting parameter ranges,

$$\frac{n_B}{s} = \frac{\xi}{D} \frac{45}{4g_*\pi^4} v_w \left(\frac{m_f}{T}\right)^2 \left(\frac{m_H}{T}\right) \Theta_{CP} \begin{cases} -\frac{\Gamma_s D_L}{v_w^2} & v_w^2 > \Gamma_\tau D_R, \Gamma_s D_L \\ +\frac{2}{3} \frac{\Gamma_s D_R}{v_w^2} & \Gamma_\tau D_R > v_w^2 > \Gamma_s D_L \\ +\frac{2}{3} & \Gamma_\tau D_R, \Gamma_s D_R > v_w^2 \\ -\frac{1}{2} \frac{v_w}{\sqrt{\Gamma_{ss} D_q}} \frac{3\Gamma_s D_q}{v_w^2} & 1 > \sqrt{\frac{v_w^2}{\Gamma_{ss} D_q}} > \frac{\delta D_q}{D_q} \\ -\frac{1}{2} \frac{\delta D_q}{D_q} \frac{3\Gamma_s D_q}{v_w^2} & \frac{\delta D_q}{D_q} > \sqrt{\frac{v_w^2}{\Gamma_{ss} D_q}}, v_w^2 > \Gamma_s D_q \end{cases} \quad (79)$$

---

<sup>†</sup> A recent study of this question [39] has developed the present analysis further quantitatively and reaches the same conclusion.



where the first three cases are for leptons and the other two for quarks. In each case  $\xi$  and  $D$  apply to the appropriate fermion (left-handed lepton in first case, right-handed lepton in following two cases, quarks in final two cases).  $\Theta_{CP}$  was defined by  $\int \mathcal{I}m[m]dz = \frac{m_f}{m_H} \Theta_{CP}$ .

As remarked earlier the mass  $m_f$  is the tree-level finite temperature mass, which we should take not to be the zero temperature mass but  $y_f \phi(T) \sim y_f T$  where  $y_f$  is the Yukawa coupling of the fermion. In particular for leptons in a two doublet model this parameter is not constrained to its standard model value by phenomenology [40].

The way we have written the result in (79) breaks it up into two pieces — an ‘injected’ piece on the left of the bracket and a ‘conversion’ factor on the right. It is clear that the leptons do much better in terms of conversion because of their much greater diffusion constants and the absence of the strong sphaleron suppression. The extra factor of three which the quarks gain is a color factor which really belongs on the left, because all three colors reflect off the barrier. The factor ended up in the conversion factor because we defined the injected flux for quarks in terms of baryon number.

In section 3 we discussed how  $Z$  could be non-zero in either a two doublet model or in the standard model if a  $Z$  condensate is formed on the wall as described in [12]. In the former case it is appropriate to take  $\Theta_{CP}$  to be simply the integrated phase change across a single bubble wall as this will be determined to be the same on every bubble wall by the effective potential, and we can take  $\Theta_{CP} \sim 1$  consistently with phenomenology.

In the  $Z$  condensate case  $\Theta_{CP}$  will contain some suppression (possibly many orders of magnitude) which will depend on the details of how one sign of the spontaneously formed condensate comes to dominate over the other as the transition is completed. This will be discussed in [33].

We note that for  $v_w^2 < \Gamma_s D$  the asymmetry goes as  $1/v_w$ . This is cut off if the weak anomalous processes have time to reach equilibrium. For velocities  $v_w < (\Gamma_s D_{l_R})^{1/2} \approx 0.75 \sqrt{\kappa_s} \alpha_w \cot^2 \theta_W$  (cf. (54) and (57)) the asymmetry goes as  $v_w$ . Note that for the right-handed leptons with their very long diffusion tail this means  $v_w < 0.1 \sqrt{\kappa_s}$  so that the third expression above can be appropriate for modest velocities. For quarks on the other hand  $v_w < (\Gamma_s D_q)^{1/2} \approx 1.2 \sqrt{\kappa_s} \alpha_w^2 / \alpha_s \sim \sqrt{\kappa_s} / 100$  requires velocities smaller than those in the calculated range  $v_w \sim 0.1 - 1$ . Recall that  $\kappa_s \sim 0.1 - 1$ .

Before using (79) to calculate some numerical values, and in order to make a detailed comparison between the cases of an injected quark flux and an injected lepton flux, we return to the conditions for the validity of (79). In writing it down we have used the injected flux which is calculated from a reflection calculation which involved various assumptions. Firstly, we solved the Dirac equation for a free fermion by expanding it perturbatively in  $m_f L_w$ . This expansion is valid provided

- *Condition 1.*  $L_w < m_f^{-1}$  (perturbative expansion)

This condition can be avoided by solving the Dirac equation exactly for a given wall profile (Higgs mass profile) and then treating the imaginary part of the mass as a perturbation (see [28], [9]). For  $L_w \gg m_f^{-1}$ , as discussed in section 3, we expect a strong WKB suppression (for typical monotonic wall ansatzes, to which we restrict ourselves).

Secondly, we treated the fermion as free on the wall. A typical particle in the injected asymmetry current has a momentum  $p_z \approx E v_z \approx m_H \approx 2/L_w$ , with typical energy  $E \sim 2T$ . The distance the particle then advances before it scatters once, given by  $v_z \gamma_f^{-1}$ ,

should be larger than the wall thickness  $L_w$ . This gives

- *Condition 2.*  $L_w < (1/T\gamma_f)^{1/2}$  (free fermion)

One might also wonder whether a more stringent condition exists - namely whether collisions occur on a length scale shorter than the de Broglie wavelength of the particles. For particles of momenta  $p_z \sim m_f$ , the de Broglie wavelength is substantially larger than  $m_H^{-1}$ , and a correct quantum treatment must include collisions. However, as noted above, the reflected asymmetric flux is dominated by over-barrier reflection of particles with momenta  $p_z \sim m_H$ , and for these Condition 2 suffices.

We note that this condition is a stronger constraint than the naive  $L_w < \gamma_f^{-1}$  which we used in section 4<sup>†</sup>. If condition 2 is not satisfied one can estimate the resultant phase space suppression.

Particles with a large incident angle on the wall ( $p_\perp \sim p_z$ ) are nonrelativistic so we can use  $p_z \approx m_f v_z \approx 2/L_w$ . The condition that these particles not scatter leads then to a weaker version of condition 2:  $L_w < (2/m_f\gamma_f)^{1/2}$ . A simple argument based on counting particles with large incident angle indicates that in this case an additional suppression of order  $1/(L_w T)^2$  to (79) will result. For the case of WKB reflection from a ‘bump’ barrier this condition is further relaxed because the reflection is dominated by thermal particles with momenta  $p_z \sim m_f$ .

Consider now whether and how the quarks and the leptons meet these conditions. First consider the *top* quark. Since its mass is so large  $m_t \sim T$ , the condition 1 requires very thin walls  $L_w < 1/T$ , which is to be compared with the perturbative value  $L_w \sim 20/T$ . Next condition 2 reads:  $L_w < 2/T$ . (The weaker version does not help since  $m_t \sim T$ .) Hence unless the wall is very thin we expect additional strong suppressions for the *top* quark which have not been included in (79).

For the leptons the conditions are much more plausibly satisfied. Take for example the right handed lepton whose long diffusion tail ends up in most cases dominating baryon production. The above conditions become: 1)  $L_w < m_{l_R}^{-1}$ ; 2)  $L_w < 9/T$ . This means that for a standard model Yukawa coupling ( $y_\tau = 0.01$ ) and a wall  $L_w \sim 10/T$  all conditions are met. The weaker version of condition 2 gives:  $L_w < 9/m_\tau^{1/2}$  so that for thicker walls we expect some phase space suppression. Note that we can allow  $y_\tau$  to vary quite a lot (consistently with the phenomenology of two Higgs doublet models) without violating the conditions.

In summary the differences between injected quark and lepton fluxes are: (i) leptons gain in ‘conversion’ in front of the wall because of their better transport properties and the absence of a strong sphaleron suppression which affects the quarks, (ii) for very thin walls  $\sim 1/T$  the ratio of the injected asymmetries in quarks and leptons is equal to the ratio of their Yukawa couplings squared, (iii) for thicker walls  $\sim 10/T$  there are suppressions for the quarks which are absent for the leptons because of their much smaller mean free path; the treatment we have presented breaks down in this case, and new techniques for computing quantum mechanical reflection in the presence of scattering are required.

Two other comments on (79) should be noted. The ‘persistence length’  $\xi$  we estimated with a naive argument to be  $6Dv_i$ , where  $v_i$  is the injected velocity. The uncertainty in

---

<sup>†</sup> We are grateful to Larry McLerran for a discussion of this point.

$\xi$  reflects the limitation of our calculation. To calculate this parameter more precisely involves going beyond the diffusion approximation to determine exactly how the reflected asymmetry sources the diffusion equation. This involves modelling how the very specific momentum space distribution of the injected flux thermalizes as it moves away from the wall. The result is clearly ansatz dependent, as was manifest in our estimate for the quantum mechanical and WKB cases (for which the appropriate  $v_i$  were quite different). For a recent study of this question and a discussion of the limitations of the diffusion approximation see [41]. Finally we recall that our diffusion approximation relied on taking  $v_w < v_s \sim 1/\sqrt{3}$ , the speed of sound in the plasma. For highly relativistic velocities the particles do not have time to thermalize before they are caught by the wall, and clearly the asymmetry will be considerably attenuated. For  $v_w > v_s$  the diffusion tail does not exist because particles cannot diffuse faster than  $v_s$ . In this case we expect local mechanisms to be the dominant sources of baryogenesis.

There is one aspect of the free particle approximation which we have not discussed - the neglect of the contribution of the thermal gauge boson excitations to the fermion self energies [42], [43]. Weldon gave a Dirac equation incorporating this and one can argue that this is the relevant equation for fermionic excitations if one is interested (as we are) in processes whose time scale is long compared to the response time of the gauge plasma  $\sim 1/gT$ , but short in comparison to the scales on which particles scatter, which is typically given by  $\sim 1/g^2T$  or  $1/g^4 \ln(1/g^2)T$  depending on particles' energy. The question of interest is then how the analysis of the reflection problem will be modified. We present in Appendix B a set of manipulations of this finite temperature Dirac equation which lead to a real space Dirac equation, the starting point for an analysis in terms of reflection coefficients. We write the equation in a form in which one can see simply how the modification of the fermion self energies at finite temperature enters. We find that the mass matrix which relates left and right handed particles becomes off-diagonal as a consequence of thermal effects. These off-diagonal elements are of order  $\alpha_w(LT)^2$  and hence small for a sufficiently thin wall. For realistic wall thicknesses however the corrections may be large and further analysis is required.

Finally we turn to the numerical evaluation of (79) in a few cases, to illustrate that our final result gives asymmetries typically compatible with the observed value. For the standard model Yukawa couplings  $m_f/T \approx y_f$  the prefactor in (79) reads  $g_*^{-1}v_w(y_f/L_wT)^2\Theta_{CP}$ , we take  $\xi = 6Dv_i$ ,  $v_i$  as given in (29),  $m_f = y_fT$  and  $2m_H^{-1} = L_w$ . In the case of the  $\tau$  lepton the first formula applies even for rather slow walls:  $v_w > 2.1y_\tau, \sqrt{\kappa_s}/20$ . In this case we find  $\frac{n_B}{s} \approx -\frac{2}{g_*} \frac{y_\tau^2}{(L_wT)^2} \frac{\kappa_s}{v_w} \alpha_w^2 \Theta_{CP}$ . If we take  $y_\tau = 0.01$  (standard model value), with  $L_wT \sim 20$ ,  $g_* = 100$  and  $v_w \sim 0.1$ , we get  $n_B/s \sim -0.6 \times 10^{-10} \kappa_s \Theta_{CP}$ , marginally compatible with the nucleosynthesis bound  $(4-7) \cdot 10^{-11}$ , provided  $CP$  violation is large  $\Theta_{CP} \sim 1$ .

The result in other regimes can be read off simply. In view of our comments above one of the most interesting regimes seems to be that of intermediate Yukawa couplings  $y_\tau \sim 0.1$ , which is described by the second case above. The answer is larger by  $3 \times 10^2$  than the case of standard model Yukawa lepton coupling. In this case we expect the reflection calculation to be reliable, as the conditions discussed above still hold. An extra factor 3 was obtained from the conversion of the injected right-handed asymmetry to baryons.

## 9. Conclusion

In this paper we have developed a new analytic formalism to treat the diffusion and decay of a chiral flux injected by reflection from a CP violating bubble wall. Our formalism allows us to fix dynamically all the injected quantum numbers rather than constrain them locally as was done in the previous calculation of this mechanism in the case of quarks. We have emphasized the case of leptons, in particular the interesting role that could be played by the right-handed leptons when the lepton Yukawa coupling is larger than its standard model value. We have also briefly examined the case of quark reflection, determining the suppression which results from strong anomalous processes.

There are many interesting issues which remain outstanding some of which we have discussed briefly (See for example [44]). The injection of the current could be modeled in a more sophisticated way [41]. Our calculations apply in the limit when the wall velocity is not relativistic, but we anticipate they should be accurate until close to the speed of sound in the plasma. It would be interesting to understand the highly relativistic case in more detail too. The ‘conversion’ will clearly be very much less efficient but some of this may be compensated for by an enhancement of the reflected asymmetry as the moving wall will be Lorentz contracted.

### Appendix A. Quantum Mechanical Reflection Coefficients

We start from equation derived in the text

$$i\partial_z \xi_{\pm} = \begin{pmatrix} \hat{E} \pm g_A Z & m \\ -m & -(\hat{E} \pm g_A Z) \end{pmatrix} \xi_{\pm} \quad S^z = \pm \frac{1}{2} \quad (80)$$

from the Lagrangian (8), in the frame in which the wall is at rest ( $Z = Z(z)$  and  $m = m(z)$ ) and in which the transverse momentum  $p_{\perp}$  has been boosted away.  $\hat{E}$  is the energy of the incident particle in this frame, related to the energy  $E$  in the unboosted frame by  $\hat{E} = \sqrt{E^2 - p_{\perp}^2}$ . We will consider particles incident on the wall ( $0 > z > z_0$ ) from the unbroken phase on the right ( $z > 0$ ). At  $z > z_0$  we take the mass to have its (real) broken phase value  $m_0$ .

We first perform the global rotation

$$\xi_{\pm} \rightarrow e^{\pm i\sigma_3 g_A \int_{z_0}^z Z dz} \xi_{\pm} \quad (81)$$

so that the redefined  $\xi_{\pm}$  obey

$$i\partial_z \xi_{\pm} = Q_{\pm} \xi_{\pm} \quad S^z = \pm \frac{1}{2} \quad (82)$$

where

$$Q_{\pm}(z) = \begin{pmatrix} \hat{E} & m_{\pm} \\ -m_{\pm}^* & -\hat{E} \end{pmatrix} \quad (83)$$

and  $m_{\pm} = m e^{\pm 2ig_A \int_{z_0}^z Z dz}$ . This is precisely the form in which the problem is analyzed by CKN in [21], an analysis which we follow until (86) below. The solution of (80) can be written

$$\xi_{\pm}(z) = P e^{-i \int_{z'}^z Q_{\pm}(z) dz} \xi_{\pm}(z') \quad (84)$$

where P indicates path ordering. The upper component of  $\xi_{\pm}$  is the left-moving eigenstate in the unbroken phase, so to describe the reflection of an incident left-handed (L) particle we put  $\xi_+(0) = \begin{pmatrix} 1 \\ \bar{r} \end{pmatrix}$  and  $\xi_+(z_0) = \bar{t}D^{-1} \begin{pmatrix} 1 \\ 0 \end{pmatrix}$ .  $D$  is the matrix which diagonalizes  $Q_{\pm} = Q_o$  in the broken phase,  $DQ_oD^{-1} = \sqrt{\hat{E}^2 - m_o^2}\sigma_3$ .  $\bar{r}$  and  $\bar{t}$  are the reflection and transmission amplitudes. We will analyze only this case, extracting the reflection coefficient for incident  $\bar{L}$  (anti-particle of  $L$ ) and incident right-handed particle  $R$  by the substitution  $m \rightarrow m^*$ . Using these definitions and the explicit form of the solution (84) we have

$$D\Omega_o \begin{pmatrix} 1 \\ \bar{r} \end{pmatrix} = \begin{pmatrix} \bar{t} \\ 0 \end{pmatrix} \quad (85)$$

where  $\Omega(z) = Pe^{-i\int_0^z Q_+(z)dz}$  and  $\Omega_o = \Omega(z_0) = \begin{pmatrix} \alpha & \beta \\ \beta^* & \alpha^* \end{pmatrix}$ , where  $\alpha, \beta$  are complex numbers to be determined.  $D$  can be obtained as  $\begin{pmatrix} c & s \\ s & c \end{pmatrix}$  where  $s = \sinh \theta$ ,  $\sinh 2\theta = \frac{m_o}{\sqrt{\hat{E}^2 - m_o^2}}$  and  $c = \cosh \theta$ ,  $\cosh 2\theta = \frac{\hat{E}}{\sqrt{\hat{E}^2 - m_o^2}}$ . We then have

$$\bar{r} = -\frac{s\alpha + c\beta^*}{s\beta + c\alpha^*}, \quad \bar{t} = \frac{1}{s\beta + c\alpha^*}. \quad (86)$$

We now define

$$U(z) = \begin{pmatrix} a & b \\ b^* & a^* \end{pmatrix} = e^{i\hat{E}\sigma_3 z}\Omega \quad (87)$$

for which

$$i\partial_z U = \begin{pmatrix} 0 & m_+^* e^{2i\hat{E}z} \\ -m_+^* e^{-2i\hat{E}z} & 0 \end{pmatrix} U \quad (88)$$

or

$$i\partial_z a = m_+ e^{2i\hat{E}z} b^* \quad i\partial_z b = m_+ e^{2i\hat{E}z} a^* \quad (89)$$

which can be integrated recursively to give

$$\begin{aligned} a &= 1 + \int_0^z m_+(z_1) e^{2i\hat{E}z_1} \int_0^{z_1} m_+^*(z_2) e^{-2i\hat{E}z_2} + \dots \\ b &= -i \left( \int_0^z m_+(z_1) e^{2i\hat{E}z_1} + \int_0^z m_+ e^{2i\hat{E}z_1} \int_0^{z_1} m_+^* e^{-2i\hat{E}z_2} \int_0^{z_2} m_+ e^{2i\hat{E}z_3} + \dots \right) \end{aligned} \quad (90)$$

Now using  $\alpha = \exp -i\hat{E}z_0 a(z_0)$  and  $\beta = \exp -i\hat{E}z_0 b(z_0)$ , expanding the expressions (86) perturbatively in the integral  $\int_0^z dz m_+(z) \exp 2i\hat{E}z$  we find, to leading order,

$$\bar{r} = -e^{-2i\hat{E}z_0} \left( t + i \int_0^{z_0} m_+ e^{-2i\hat{E}(z-z_0)} + it^2 \int_0^{z_0} m_+^* e^{+2i\hat{E}(z-z_0)} \right) \quad (91)$$

where  $t = \tanh \theta$  ( $\tanh 2\theta = \frac{m_0}{E}$ ). Squaring to find the reflection probability

$$\begin{aligned} R_{L \rightarrow R} &= |\bar{r}|^2 = t^2 - it(1-t^2) \left( \int_0^{z_0} dz m_+^* e^{2i\hat{E}(z-z_0)} - \int_0^{z_0} dz m_+ e^{-2i\hat{E}(z-z_0)} \right) \\ &= t^2 + t(1-t^2) \left( 2 \int_0^{z_0} \mathcal{R}e(m_+) \sin 2i\hat{E}(z-z_0) - 2 \int_0^{z_0} \mathcal{I}m(m_+) \cos 2i\hat{E}(z-z_0) \right) \end{aligned} \quad (92)$$

Thus, using the replacement  $m \rightarrow m^*$  for anti-particles, we obtain the leading term for the difference in reflection coefficients incident with momentum  $p_z = p_z(+\infty) = \hat{E}$ :

$$\mathcal{R}(p_z) \equiv R_{L \rightarrow R} - R_{\bar{L} \rightarrow \bar{R}} = -\frac{4t(1-t^2)}{|m_0|} \int_{-\infty}^{\infty} \mathcal{I}m[m(z)m_0^*] \cos(2p_z z) dz. \quad (93)$$

This formula should be treated with caution as at next order in the perturbative expansion there is a  $t$ -independent term

$$2 \int_0^{z_0} dz_1 \int_0^{z_0} dz_2 \mathcal{I}m[m_+^*(z_1)m_+(z_2)] \sin 2p_z(z_1 - z_2). \quad (94)$$

Clearly the approximation (93) is only valid provided  $t$  is not so small that (93) is smaller than (94). In the cases we actually apply (93) this is only a marginal approximation.

### Appendix B. Finite temperature plasma effects

The one loop finite temperature corrected dispersion relation for fermions in a hot gauge plasma was firstly discussed by Klimov in Ref. [42]. Here we follow Ref. [43] which gives a Dirac equation in momentum space which may be written

$$[(1+a)\not{P} + b\not{u} - m] \Psi = 0 \quad (95)$$

where  $P^\mu$  is the four-momentum of a particle and  $u^\mu$  is the four-velocity of the plasma. In the plasma frame  $u^\mu = (1, \vec{0})$ , while in the wall frame  $u^\mu = (\gamma_w, -\gamma_w \vec{v}_w)$ , and  $m$  is the tree-level mass of the particle. For  $\omega < T$ ,  $p < T$  the coefficients  $a$  and  $b$  read:

$$a_{L,R} = \frac{M_{L,R}^2}{p^2} \left[ 1 - \frac{\omega}{2p} \ln \frac{\omega+p}{\omega-p} \right], \quad b_{L,R} = \frac{M_{L,R}^2}{p} \left[ -\frac{\omega}{p} + \left( \frac{\omega^2}{p^2} - 1 \right) \frac{1}{2} \ln \frac{\omega+p}{\omega-p} \right], \quad (96)$$

where  $M_L$  and  $M_R$  are the one-loop finite temperature corrected left- and right-handed fermion masses, and  $\omega = P^\mu u_\mu$ ,  $p = [\omega^2 - P^\mu P_\mu]^{1/2}$  [43]. Since we are mainly interested in studying thermal particles with  $\omega, p \geq T$  we have evaluated the integrals (A4) – (A5) in [43] and found that the relevant change to  $a$  and  $b$  is:  $\ln(\omega+p) \rightarrow \ln \zeta T$ , where  $\zeta \simeq 1-2$ .

The thermal masses for the left-handed ( $qL$ ), right-handed  $up$  ( $uR$ ) and right handed  $down$  ( $dR$ ) quarks [43] are

$$\begin{aligned} M_{qL}^2 &= \frac{2}{3} \pi \alpha_s T^2 + \frac{3}{8} \pi \alpha_w T^2 + \frac{1}{72} \pi \alpha_w \tan^2 \theta_W T^2 \\ M_{uR}^2 &= \frac{2}{3} \pi \alpha_s T^2 + 0 + \frac{2}{9} \pi \alpha_w \tan^2 \theta_W T^2 \\ M_{dR}^2 &= \frac{2}{3} \pi \alpha_s T^2 + 0 + \frac{1}{18} \pi \alpha_w \tan^2 \theta_W T^2 \end{aligned} \quad (97)$$

while for the leptons

$$\begin{aligned} M_{lL}^2 &= 0 + \frac{3\pi}{8}\alpha_w T^2 + \frac{\pi}{8}\alpha_w \tan^2 \theta_W T^2 \\ M_{lR}^2 &= 0 + 0 + \frac{\pi}{2}\alpha_w \tan^2 \theta_W T^2. \end{aligned} \quad (98)$$

For both quarks and leptons

$$M_L^2 - M_R^2 \simeq \frac{3\pi}{8}\alpha_w T^2 \quad (99)$$

We incorporate the effect of a classical axial field  $Z_\mu$  in (95) by a canonical replacement:

$$\mathcal{P} \rightarrow \mathcal{P} - g_A \mathcal{Z} \gamma_5 \quad (100)$$

since the  $Z$  field couples axially. We wish to answer the question of how much the results for the reflection calculation deviate from the free particle case studied in the main text and in Appendix A. Our analysis will be far from exhaustive. We will content ourselves with showing that the corrected Dirac equation can be written with some simple assumptions in a form which is manifestly that of the free particle case, with corrections which are small.

We consider as in the text a one-dimensional wall lying in the  $xy$  plane. In order to study the reflection problem we need to return to a real space Dirac equation. We do so by replacing  $P_z \rightarrow -i\partial_z$  and making the following assumption: we assume  $a$  and  $b$  in (95) to be well approximated as scalar functions of  $\omega$  by taking  $p = p(\omega)$  in (96). This is true in the leading order of a derivative expansion in the background fields i.e. in the WKB limit. Here we are however interested in the quantum-mechanical momenta  $P_z$  typically of precisely the inverse length scale  $L^{-1}$  of the variation in the background. Since  $p \sim [P_\perp^2 + P_z^2]^{1/2} \rightarrow [P_\perp^2 - \partial_z^2]^{1/2}$  this assumption should be valid provided  $p \gg L^{-1}$  which will be true for the thermal particles we wish to describe. As long as we restrict ourselves to particles incident at small glancing angles (which dominate phase space) our real  $z$ -space equation should apply.

We start by re-writing (95) (with  $Z$  field included) for the two component right-handed  $\Psi_R$  and left-handed  $\Psi_L$  spinors in the chiral representation (in which  $\Psi \sim [\Psi_R, \Psi_L]$ )

$$\begin{aligned} [i\partial_z - g_A Z] \Psi_R &= \sigma_3 \left[ (\hat{E} + c_R \hat{u}^0) - c_R \vec{\sigma} \cdot \hat{\vec{u}} \right] \Psi_R + \sigma_3 m_R(z) \Psi_L \\ [i\partial_z + g_A Z] \Psi_L &= \sigma_3 \left[ -(\hat{E} + c_L \hat{u}^0) - c_L \vec{\sigma} \cdot \hat{\vec{u}} \right] \Psi_L - \sigma_3 m_L(z) \Psi_R \end{aligned} \quad (101)$$

where we used  $\gamma_5 \Psi_{R,L} = \pm \Psi_{R,L}$ . As in the free case we are again working in the wall frame in which we have transformed away the momentum  $\vec{P}_\perp$  parallel to the wall by a Lorentz transformation

$$\hat{\vec{P}}_\perp = \gamma_\perp (\vec{P}_\perp - \vec{v}_\perp E) = 0 \quad (102)$$

such that

$$\vec{v}_\perp = \frac{\vec{P}_\perp}{E}, \quad \gamma_\perp = \frac{E}{\hat{E}}, \quad \hat{E} = \sqrt{E^2 - P_\perp^2} \quad (103)$$

and

$$\hat{u}^0 = \gamma_\perp u^0, \quad \hat{\vec{u}}_\perp = -\gamma_\perp \vec{v}_\perp u^0 \quad (104)$$

Recall that  $Z^\mu = (0, 0, 0, Z(z))$  and  $u^\mu = (u^0, 0, 0, u_3)$  ( $u^0 = \gamma_w$ ,  $u_3 = -\gamma_w v_w$ ) are the field and the velocity of plasma in the wall frame. As a last step to obtaining (101) we have divided (95) by  $(1 + a_{L,R})$  so that

$$m_{R,L}(z) = \frac{m(z)}{1 + a_{R,L}}, \quad c_{R,L} = \frac{b_{R,L}}{1 + a_{R,L}} \quad (105)$$

Note that (101) is more complicated than the corresponding free particle one since the chirality eigenstates  $\Psi_{R,L} = \begin{pmatrix} 1 \\ 0 \end{pmatrix}$  and  $\Psi_{R,L} = \begin{pmatrix} 0 \\ 1 \end{pmatrix}$  are no longer the eigenstates of the Dirac operator in the massless limit. Indeed the term

$$-c_{R,L} \sigma_3 \vec{\sigma} \cdot \hat{\vec{u}} \quad (106)$$

mixes the state  $\begin{pmatrix} 1 \\ 0 \end{pmatrix}$  with  $\begin{pmatrix} 0 \\ 1 \end{pmatrix}$ . To find the true momentum eigenstates one diagonalizes the the Dirac operator:

$$\begin{aligned} \mathcal{D}_R &= \sigma_3 \left[ (\hat{E} + c_R \hat{u}^0) - c_R \vec{\sigma} \cdot \hat{\vec{u}} \right] \\ \mathcal{D}_L &= \sigma_3 \left[ -(\hat{E} + c_L \hat{u}^0) - c_L \vec{\sigma} \cdot \hat{\vec{u}} \right] \end{aligned} \quad (107)$$

This induces a nontrivial transformation on  $m_R$  and  $m_L$  and they become non-diagonal matrices, *i.e.* a pure right-handed (left-handed) travelling wave couples *via* plasma effects to both components of the left-handed (right-handed) travelling wave (in the presence of a non-zero tree level mass).

The momentum eigenvalues for the right-handed particles are

$$P_z \equiv \lambda_R^{(\pm)} = -c_R u_3 \pm \left[ (\hat{E} + c_R \hat{u}^0)^2 - c_R^2 \hat{u}_\perp^2 \right]^{\frac{1}{2}} \equiv -c_R u_3 \pm \lambda_R \quad (108)$$

and similarly for the left-handed fermions, with index  $R \rightarrow L$ . It is trivial to re-write these relations in the plasma frame (in which  $u^\mu = (1, 0, 0, 0)$ )

$$P_z = \pm \left[ (E + c_R)^2 - P_\perp^2 \right]^{\frac{1}{2}}, \quad P_z = \pm \left[ (E + c_L)^2 - P_\perp^2 \right]^{\frac{1}{2}} \quad (109)$$

Note that the high momentum limit ( $P \gg M$ ) of these are

$$E^2 = P^2 + 2M_R^2, \quad E^2 = P^2 + 2M_L^2 \quad (110)$$

Roughly speaking thermal particles in plasma ( $P \sim T$ ) behave as free particles with mass squared equal  $2M_{R,L}^2$  *plus* the tree level mass squared, with the important difference that plasma mass does not mix chiralities



Having found the eigenvalues (108) for  $\mathcal{D}_{R,L}$ , it is now straightforward to construct the matrix that diagonalizes them

$$\mathcal{R}_R = \left( \frac{\hat{E} + c_R \hat{u}^0}{\lambda_R} \right)^{\frac{1}{2}} \left[ v_R^{(+)}, v_R^{(-)} \right] \quad (111)$$

where  $v_R^{(\pm)}$  are the eigenvectors which correspond to  $\lambda_R^{(\pm)}$

$$\begin{aligned} v_R^{(+)} &= \mathcal{N}_R \begin{pmatrix} \hat{E} + c_R \hat{u}^0 + \lambda_R \\ c_R(\hat{u}^1 + i\hat{u}^2) \end{pmatrix}, & v_R^{(-)} &= \mathcal{N}_R \begin{pmatrix} c_R(\hat{u}^1 - i\hat{u}^2) \\ \hat{E} + c_R \hat{u}^0 + \lambda_R \end{pmatrix} \\ \mathcal{N}_R^{-2} &= 2(\hat{E} + c_R \hat{u}^0)(\hat{E} + c_R \hat{u}^0 + \lambda_R) \end{aligned} \quad (112)$$

and similarly for the left-handed particles. We can now use  $\mathcal{R}_{R,L}$  to diagonalize  $\mathcal{D}_{L,R}$ :

$$\begin{aligned} \mathcal{R}_R^{-1} \mathcal{D}_R \mathcal{R}_R &= \text{diag}(-c_R \hat{u}^0 + \lambda_R, -c_R \hat{u}^0 - \lambda_R) \equiv d_R \\ \mathcal{R}_L^{-1} \mathcal{D}_L \mathcal{R}_L &= \text{diag}(-c_L \hat{u}^0 - \lambda_L, -c_L \hat{u}^0 + \lambda_L) \equiv d_L \end{aligned} \quad (113)$$

so that the left moving particles (negative eigenvalue) correspond in this new basis to  $\begin{pmatrix} 0 \\ 1 \end{pmatrix}$  for the right-handed particles and  $\begin{pmatrix} 1 \\ 0 \end{pmatrix}$  for the left-handed particles and *vice versa* for the right movers (with positive eigenvalues).

Now (101) can be recast as

$$\begin{aligned} [i\partial_z - g_A Z] \check{\Psi}_R &= d_R \check{\Psi}_R + m_R(z) \mathcal{K}_0 \check{\Psi}_L \\ [i\partial_z + g_A Z] \check{\Psi}_L &= d_L \check{\Psi}_L - m_L(z) \mathcal{K}_0^{-1} \check{\Psi}_R \end{aligned} \quad (114)$$

where we have defined  $\mathcal{R}_R^{-1} \Psi_R = \check{\Psi}_R$ .  $\mathcal{K}_0$  is an approximately diagonal mass matrix

$$\mathcal{K}_0 = \mathcal{R}_R^{-1} \sigma_3 \mathcal{R}_L = \kappa_0 \sigma_3 - \eta \sigma_3 \vec{\sigma} \cdot \hat{u}_\perp \quad (115)$$

Indeed one can check that

$$\kappa_0 = 1 + o(\Delta c)^2, \quad \eta \simeq \frac{\Delta c}{2(\hat{E} + c)} (1 + o(c)) \quad (116)$$

In order to make a comparison with the free particle case we rotate the spinors in (114) one more time as follows:

$$\check{\Psi}_R \rightarrow \tilde{\Psi}_R = e^{i \int g_A Z dz} e^{i d_R z} \check{\Psi}_R, \quad \check{\Psi}_L \rightarrow \tilde{\Psi}_L = e^{-i \int g_A Z dz} e^{i d_L z} \check{\Psi}_L \quad (117)$$

so that (114) reduce to

$$i\partial_z \tilde{\Psi}_R = m_R(z) e^{2i \int g_A Z dz} \mathcal{K} \tilde{\Psi}_L, \quad i\partial_z \tilde{\Psi}_L = -m_L(z) e^{-2i \int g_A Z dz} \mathcal{K}^{-1} \tilde{\Psi}_R \quad (118)$$

where

$$\mathcal{K} = e^{id_R z} \mathcal{K}_0 e^{-id_L z} = e^{i\Delta c u_3 z} \begin{pmatrix} e^{2i\lambda z} & -\eta e^{2i\lambda z}(\hat{u}_1 - i\hat{u}_2) \\ \eta e^{-2i\lambda z}(\hat{u}_1 + i\hat{u}_2) & -e^{-2i\lambda z} \end{pmatrix} \quad (119)$$

Where  $\lambda^2 = (\hat{E} + c)^2 - c^2 \hat{u}_\perp^2$ . The matrix  $\mathcal{K}$  is diagonal for free particles (when  $T = 0$ ) and equals  $\sigma_3$ . The deviation is due to thermal effects and it is of order  $\eta \hat{u}_\perp \sim \alpha_w (TL)^2$ . This is small for a sufficiently thin wall, such as we concentrate on here, but  $O(1)$  or greater for thicker realistic walls. We leave a fuller analysis of the effects of these corrections to future work.

### Appendix C: Diffusion Constant Calculations

To calculate the diffusion constant we generalize the method outlined in [45]. In the companion paper we present an alternative derivation based on a local thermal equilibrium *ansatz* for the distribution function, which yields a very similar result.

We focus on the elastic scattering,  $t$ -channel vector boson exchange diagrams, which are expected to dominate the scattering process, and play the major role in limiting the diffusion of particles (the divergence in the propagator as  $t \sim M^2$ , where  $M$  is the mass of the exchanged vector boson, leads to a logarithmic enhancement of the scattering rate).

The diffusion constant  $D$  measures the particle number current induced by a gradient in the number density:

$$\vec{J}_d = -D \nabla n \quad (120)$$

where  $J_d$  is the diffusion (number density) current,  $n$  number density. We calculate  $D$  by considering a steady state situation in which some external source and sink cause the particle number density to vary slowly with  $x$ . To a first approximation, the distribution function is just  $f_0 = 1/[\exp(\beta E + \xi) + 1]$  (where  $\beta = 1/T$  is the inverse temperature,  $E = p^0$  the energy, and  $\xi$  the chemical potential), and  $\xi$  varies slowly with  $x$ . This distribution function however has no current, so we compute the deviation  $\delta f$  in the distribution function  $f = f_0 + \delta f$ , by solving the Boltzmann equation, and then compute the current from

$$\vec{J} = \int \vec{d}^3 p \delta f \frac{\vec{p}}{E} \quad (121)$$

The perturbation  $\delta f$  is of order  $\tau/l$  where  $\tau$  is the mean free path and  $l$  the length scale over which  $\xi$  varies: the calculation is accurate in the regime where  $\tau/l \ll 1$ .

We determine  $\delta f$  from the static Boltzmann equation, which reduces to

$$d_t f = \frac{\vec{p}}{p^0} \cdot \nabla_{\vec{x}} f = -C(f), \quad (122)$$

Expanding the collision integral  $C(f)$  in terms of  $\delta f$  and expressing the *L.H.S.* of (122) in terms of  $\nabla_{\vec{x}} n$ , we find the relation (120) from which we read off the constant  $D$ .

The collision integral for two *in*-coming  $\{p^\mu, k^\mu\}$  and two *out*-going particles  $\{p'^\mu, k'^\mu\}$ :

$$C(f) = \frac{1}{2p^0} \int_{\{p', k, k'\}} \delta^4(\Sigma p_i) |\mathcal{M}|^2 \mathcal{P}[f], \quad (123)$$

$$\mathcal{P}[f] = f_p f_k (1 - f_{p'}) (1 - f_{k'}) - f_{p'} f_{k'} (1 - f_p) (1 - f_k)$$

where  $\delta^4(\sum p_i)$  ensures the energy-momentum conservation,  $\int_p = \int \vec{d}^3 p / 2p^0$ , and  $\mathcal{M}$  stands for the appropriate scattering amplitude. For particles exchanging  $B$  vector bosons (corresponding to the  $U(1)_Y$  symmetry),  $W$  bosons ( $SU(2)_L$ ) and  $g$  gluons ( $SU(3)_c$ ), the amplitudes are

$$\begin{aligned} |\mathcal{M}_B|^2 &= 80Y^2 g_1^4 \frac{s^2}{(t - M_B^2)^2} \\ |\mathcal{M}_W|^2 &= 36g_2^4 \frac{s^2}{(t - M_W^2)^2} \\ |\mathcal{M}_g|^2 &= 32g_3^4 \frac{s^2 + u^2}{(t - M_g^2)^2} \end{aligned} \quad (124)$$

where  $Y$  is the hypercharge of the particle we are following (in the convention  $Q = T^3 + Y$ ),  $g_1$ ,  $g_2$  and  $g_3$  are the  $U(1)_Y$ ,  $SU(2)_L$  and  $SU(3)_c$  gauge couplings, with  $g_1 = g_2 \tan \theta_W$ ,  $s = (p+k)^2 = 2p \cdot k$ ,  $t = (p-p')^2 = -2p \cdot p'$ ,  $u = (p-k')^2 = -2p \cdot k'$  and  $\sin^2 \theta_W = 0.23$ ,  $\theta_W$  is the Weinberg angle. Note that in calculating (124) we have set masses of all particles at the outer legs to zero. This is justified since we are interested in leading order ( $g^4$ ) contribution to the scattering amplitudes. The  $t$ -channel processes possess a logarithmic divergence when integrated over the momenta if the exchange particle is massless. One can cure this divergence by using the thermally corrected gluon propagator. Since in the approximation when the scattering particles are massless and on shell,  $t \leq 0$ , the gluon is Debye screened. To the leading-log accurate one can use for the propagator  $g_{\mu\nu}/(t - M_g^2)$ , where  $M_g(T)$  is the Debye mass. In this approximation the dominant contribution to the scattering integral comes from the particles with the exchange momenta of order  $M_g$ . Note that so far we have not addressed the question of the difference between the longitudinal and transverse bosons. We suspect that the contribution from the transverse bosons, which are not Debye screened at the one-loop level, is larger, but since we do not know what is the appropriate screening mass, we will treat all exchange bosons equally, as if they were longitudinal. The (one-loop) Debye masses of the (longitudinal) gauge bosons are:  $M_B^2 = \frac{4\pi}{3} \alpha_w \tan^2 \theta_W T^2 \approx 0.04T^2$ ,  $M_W^2 = \frac{20\pi}{3} \alpha_w T^2 \approx 0.69T^2$ ,  $M_g^2 = 8\pi \alpha_s T^2 \approx 3.6T^2$  [43], where we wrote  $\alpha_w = g_2/4\pi$ ,  $\alpha_s = g_3/4\pi$ . Note that the gluon thermal mass is rather large: this means that the leading logarithm approximation calculation (which relies on an expansion in  $M/T$ ) may be not very accurate.

For the local equilibrium distribution functions,  $\mathcal{P}[f_0] = 0$  in (123) so that  $C(f) = 0$ , a consequence of the energy conservation  $p^0 + k^0 = p'^0 + k'^0$ . Now we make our key approximation — we assume that there is little energy transferred in a collision, so that  $p \approx p'$ , which implies  $k \sim k'$ . For light exchange bosons this is quite a good approximation. Nevertheless even for exchange of rather heavy gluons, this is true on average, since a particle is just as likely to gain as to lose energy in a collision. With this, we find to first order in  $\delta f$ ,  $\mathcal{P}[f] \approx (\delta f_{\vec{p}} - \delta f_{\vec{p}'}) (f_k^0 (1 - f_k^0))$ , where we ignore the fluctuations in the second fluid  $\delta f_k$ ,  $\delta f_{k'}$ .

If locally particle concentration varies in  $x$  direction, then the *L.H.S.* of (122) becomes  $\frac{p_x}{p^0} \partial_x \xi(x) f'$ , where  $f' = \partial f / \partial (\beta p^0 + \xi)$ . This motivates the *Ansatz*

$$\delta f_{\vec{p}} = g(p, x) \frac{p_x}{p^0} \quad (125)$$

so that  $\delta f_{\vec{p}'} = g(p') \frac{p'_x}{p'^0} \approx g(p) \frac{p_x}{p^0} \cos \alpha$ , where  $\cos \alpha = \vec{p} \cdot \vec{p}' / pp' \approx \vec{p} \cdot \vec{p}' / p^2$ .

The Boltzmann equation (122), (123) can be now recast as

$$\begin{aligned} f'_p \partial_x \xi &\approx -g(p) \Gamma_t \\ \Gamma_t &= \frac{1}{2(p^0)^3} \int_{\{p', k, k'\}} \delta^4(\sum p_i) |\mathcal{M}|^2 (-f') p \cdot p' \end{aligned} \quad (126)$$

Finally using (120), (121), and (126), with  $n \approx n_0 - T^3 \xi / 12$ , we find

$$D = \frac{12}{T^3} \int \bar{d}^3 p \frac{-f'_p}{\Gamma_t} \left( \frac{p_z}{p^0} \right)^2 \quad (127)$$

The integration required for  $\Gamma_t$  is simple when one notices that the integrand of the  $k'$ , and  $p'$  integrals is Lorentz invariant and can therefore be performed in the center of mass ( $CM$ ) frame, in which  $\vec{p} + \vec{k} = 0 = \vec{p}' + \vec{k}'$ ,  $p^0 = k^0$ ,  $p'^0 = k'^0$ . We compute to leading order in  $M/T$ , obtaining for example for the gluon exchange case

$$\Gamma_t \approx \frac{1}{6\pi} \frac{T^3}{p^2} \ln\left(\frac{4pTx_2}{M^2}\right) \quad (128)$$

The diffusion constant follows immediately from (127):

$$\begin{aligned} D_B^{-1} &\approx \frac{100}{7\pi} \alpha_w^2 \tan^4 \Theta_W Y^2 T \ln\left(\frac{32T^2}{M_B^2}\right) \\ D_W^{-1} &= \frac{45}{7\pi} \alpha_w^2 T \ln\left(\frac{32T^2}{M_W^2}\right) \\ D_G^{-1} &= \frac{80}{7\pi} \alpha_s^2 T \ln\left(\frac{32T^2}{M_G^2}\right) \end{aligned} \quad (129)$$

keeping the leading order logarithms. (We evaluated the integrals containing *logarithms* using  $\int x^n f'_x \ln(1/x) \approx \ln(1/x_n) \int x^n f'_x$ , where  $x_n \approx n$  is the value which maximizes  $x^n f'_x$ . This is quite a good approximation because  $\ln(1/x)$  varies slowly where  $x^n f'_x$  is large.) These considerations lead to the following diffusion constants for the right- and left-handed leptons and quarks

$$\begin{aligned} D_{l_R}^{-1} &= D_B^{-1} \approx \frac{T}{380} \\ D_{l_L}^{-1} &= D_W^{-1} + \frac{1}{4} D_{l_R}^{-1} \approx \frac{T}{100} \\ D_{q_{L,R}}^{-1} &= Y_{q_{L,R}}^2 D_{l_R}^{-1} + \epsilon_{L,R} D_W^{-1} + D_g^{-1} \approx \frac{T}{6} \end{aligned} \quad (130)$$

where for the coupling constants we have used  $\alpha_w \tan^2 \Theta_W = 1/103$ ,  $\alpha_w = 1/30$ ,  $\alpha_s = 1/7$ , and for the logarithms involving  $M_B$ ,  $M_W$  and  $M_G$ , the values 6.1, 3.8, 2.2 respectively.  $\epsilon_L = 1$  and  $\epsilon_R = 0$  take care of the fact that the right handed quarks do not couple to the

$W$  boson. To get a feeling how good is the expansion in  $(M/T)^2$  we have also evaluated the next (mass independent) term and got a correction to the leading logarithm:  $3/2, 3/2, 9/4$  for the  $B, W$  and gluon exchange respectively, which indicates that, except perhaps for the gluon case case, this expansion is a rather good one.

### Appendix D: Calculation of Decay Rates

In this Appendix we outline the calculation of the decay rates due to fermion/Higgs and Higgs exchange processes shown in Figures 3 and 4.

The rate per particle per unit time can be defined in the real time formalism as the integrated scattering amplitude squared in a thermal bath of particles:

$$\Gamma = \frac{12}{T^3} \int_{\{p,p',k,k'\}} f_p \tilde{f}_k (1 + \tilde{f}_{p'}) (1 - f_{k'}) \delta^4(p + k - p' - k') |\mathcal{M}|^2 \quad (131)$$

Factor  $12/T^3 = \mu/n_0 T$  ( $\mu$  is the chemical potential and  $n_0$  number density for a single species) converts the rate per unit volume and time into the rate per unit time (see (32)). In the above  $\int p = \int \tilde{d}^3 p / 2E_p$ ;  $f_p$  and  $\tilde{f}_k$  are the distribution functions for the *in*-going fermion and boson;  $(1 + \tilde{f}_{p'})$  and  $(1 - f_{k'})$  are the spin blocking for the *out*-going particles. We assume thermal distributions for particles; if not thermal, the appropriate distribution functions should be used.

First we focus on the calculation of the fermion/Higgs rate. The scattering amplitudes squared for an *in*-coming left-handed, right-handed lepton and a quark are:

$$\begin{aligned} |\mathcal{M}_{l_R}|^2 &= 2|\mathcal{M}_{l_L}|^2 = (A_W + \frac{1}{4}A_B) \frac{-ts}{(t - m_{l_L}^2)^2} + A_B \frac{-ts}{(t - m_{l_R}^2)^2} \\ |\mathcal{M}_q|^2 &= A_q \frac{-ts}{(t - m_q^2)^2} \end{aligned} \quad (132)$$

where the constants are for a  $B$ -boson (on external leg)  $A_B = 16\pi\alpha_w \tan^2 \theta_W y_l^2$ , for a  $W$ -boson  $A_W = 24\pi\alpha_w y_l^2$ , and for a gluon  $A_q = \frac{128}{3}\pi\alpha_s y_q^2$ , ( $\theta_W =$  Weinberg angle,  $y$ 's = Yukawa couplings,  $\alpha_w = 1/30$ ,  $\alpha_W \tan^2 \theta_W = 1/103$ ). For fermion masses we take the one-loop thermal values:  $m_{l_R} = 0.13T$ ,  $m_{l_L} = 0.33T$ ,  $m_q = 0.88T$ . To evaluate the integral in (131) the expression we need to integrate is

$$\begin{aligned} \Gamma &= \frac{12}{T^3} \int_{p,k} f_p \tilde{f}_k \mathcal{I} \\ \mathcal{I} &= \int_{p',k'} \delta^4(p + k - p' - k') A \frac{-ts}{(t - m^2)^2} \end{aligned} \quad (133)$$

By ignoring the spin blocking we overestimate the rate by a factor 1–4. (The spin blocking has a value in  $[1/4, 1]$  for any momenta  $\vec{p}, \vec{k}$ , and it is approximately *one* ( $\sim (1 - 2/e^3)$ ) for thermal momenta  $\sim 3T$ .)  $\mathcal{I}$  can be easily evaluated in the  $CM$  frame (see Appendix C)

$$\mathcal{I} = \frac{A}{8\pi} \left[ \ln\left(1 + \frac{2p \cdot k}{m^2}\right) - 1 + \frac{1}{1 + \frac{2p \cdot k}{m^2}} \right] \quad (134)$$

The integrals over  $p$  and  $k$  we approximate using:

$$\eta_m(n) = \int dx x^m e^{nx} \ln x = \frac{m!}{n^{m+1}} \left[ 1 + \frac{1}{2} + \dots + \frac{1}{m} - \mathcal{C} - \ln n \right] \quad (135)$$

$$\int dx x^m f_x \ln \frac{1}{x} \approx \ln \frac{1}{x_{m+1}} \int dx x^m f_x,$$

( $\mathcal{C} = 0.577$  is the Euler constant,  $x_{m+1} \approx m + 1$ ) and obtain the rate per unit time:

$$\Gamma = \frac{\zeta_3 AT}{64\pi^3} \left[ \ln \left( \frac{4x_2 T^2}{m^2} \right) - 2 - \frac{1}{\zeta_3} \sum_n \eta_1(n) \right] \quad (136)$$

This estimate together with (132) gives the following rates for right-handed, left-handed leptons and quarks

$$\Gamma_{LR} \equiv \Gamma_{l_R} = 2\Gamma_{l_L} =$$

$$\frac{3\zeta_3}{8\pi^2} \alpha_w y_l^2 \left[ \left( 1 + \frac{1}{6} \tan^2 \theta_W \right) \ln \frac{4x_2 T^2}{m_{l_L}^2} + \frac{2}{3} \tan^2 \theta_W \ln \frac{4x_2 T^2}{m_{l_R}^2} \right] T \approx 0.28 \alpha_w y_l^2 T$$

$$\Gamma_q = \frac{2\zeta_3}{3\pi^2} \alpha_s y_q^2 \ln \frac{4x_2 T^2}{m_{q_R}^2} T \approx 0.19 \alpha_s y_q^2 T \quad (137)$$

In order to obtain the approximate expressions for  $\Gamma$ 's in (137) we have used  $\tan^2 \theta_W = 0.29$ , and the standard one-loop formula for thermal masses of fermions  $m^2 = g^2 C_R T^2 / 8$  ( $C_R$  is the Casimir constant for representation  $R$ ). This gives  $m_{l_R} = 0.13T$ ,  $m_{l_L} = 0.33T$ ,  $m_q = 0.88T$ , so that the corresponding logarithms are  $\ln(8T^2/m_{l_R}^2) = 6.3$ ,  $\ln(8T^2/m_{l_L}^2) = 4.3$ ,  $\ln(8T^2/m_{q_R}^2) = 2.3$  ( $x_2 \approx 2$ ).

The third family rates are fastest ( $\tau$  lepton and *top* quark) because of their large Yukawa couplings.

In order to evaluate the Higgs exchange diagram (Fig. 4) we need the scattering amplitudes:

$$|\mathcal{M}|^2 = A \frac{t^2}{(t - m_H^2)^2} \quad (138)$$

where  $A$  takes account of coupling constants and counting. Some care is required to count the diagrams for quarks and leptons. If one assumes that *all* fermions couple to the same Higgs (just like in the standard model) for the third family one gets

$$\begin{aligned} A_{t_L} &= A_{b_L} = 12y_t^2 y_b^2 + 2(y_t^2 + y_b^2) y_\tau^2 + \text{other families} \\ A_{t_R} &= 12y_t^2 y_b^2 + 4y_t^2 y_\tau^2 + \text{other families} \\ A_{b_R} &= 12y_t^2 y_b^2 + 4y_b^2 y_\tau^2 + \text{other families} \\ A_{\tau_R} &= 2A_{\tau_L} = 12(y_t^2 + y_b^2) y_\tau^2 + \text{other families} \end{aligned} \quad (139)$$

We now integrate (135) for the Higgs exchange process in the  $CM$  frame. The only difference in the scattering amplitude is  $(-s) \rightarrow t$ :

$$\mathcal{I}' = \frac{A}{8\pi} \left[ 1 - \frac{m^2}{p \cdot k} \ln \left( 1 + \frac{2p \cdot k}{m^2} \right) + \frac{1}{1 + \frac{2p \cdot k}{m^2}} \right] \quad (140)$$

We can then approximate the integrals over  $\vec{p}$  and  $\vec{k}$  by expanding in  $(m/T)^2$ . The leading order term gives

$$\Gamma = \frac{AT}{512 \cdot 3\pi} \quad (141)$$

Taking account of counting (139) we finally obtain the rates for third family:

$$\begin{aligned} \Gamma_{t_L} = \Gamma_{b_L} &= \frac{T}{128\pi} \left[ y_t^2 y_b^2 + \frac{1}{6} (y_t^2 + y_b^2) y_\tau^2 \right] + \text{other families} \\ \Gamma_{t_R} &= \frac{T}{128\pi} \left[ y_t^2 y_b^2 + \frac{1}{3} y_t^2 y_\tau^2 \right] + \text{other families} \\ \Gamma_b &= \frac{T}{128\pi} \left[ y_t^2 y_b^2 + \frac{1}{3} y_b^2 y_\tau^2 \right] + \text{other families} \\ \Gamma_{\tau_R} = 2\Gamma_{\tau_L} &= \frac{T}{128\pi} [(y_t^2 + y_b^2) y_\tau^2] + \text{other families} \end{aligned} \quad (142)$$

These rates are model dependent. Indeed if one takes perhaps by particle physics a more motivated case in which one Higgs couples to the *up* type of quarks and the other to the *down* type and leptons, the terms  $y_t^2 y_b^2$  and  $y_t^2 y_\tau^2$  in (142) drop, altering the rate.

### Acknowledgements

We thank K. Kainulainen, L. McLerran and M. Shaposhnikov for discussions. We thank the Isaac Newton Institute, Cambridge, U.K. for hospitality while this work was being completed. The work of N.T. and T.P. was partially supported by NSF contract PHY90-21984, and the David and Lucile Packard Foundation. M.J. is supported by a Charlotte Elizabeth Procter Fellowship.

## References

- [1] For reviews see N. Turok, in *Perspectives in Higgs Physics*, ed. G. Kane, publ. World Scientific, p. 300(1992); A. Cohen, D. Kaplan and A. Nelson, *Ann. Rev. Nucl. Part. Phys.* **43** 27(1993).
- [2] G. 't Hooft, *Phys. Rev. Lett.* **37**, 8 (1976); V. Kuzmin, V. Rubakov and M. Shaposhnikov, *Phys. Lett.* **155B**, 36 (1985); F. Klinkhamer and N. Manton, *Phys. Rev.* **D30**, 2212 (1984); P. Arnold and L. McLerran, *Phys. Rev.* **D37**, 1020.
- [3] M. Dine, P. Huet, R. Leigh and A. Linde, *Phys. Lett.* B283 (1992) 319; *Phys. Rev. D* 46 (1992) 550.
- [4] B. Bunk, E.-M. Ilgenfritz, J. Kripfganz and A. Schiller, *Phys. Lett.* **B284**, 371 (1992); *Nuc. Phys.* **B403**, 453 (1993).
- [5] M. Dine and J. Bagnasco, *Phys. Lett.* B303 (1993) 308.
- [6] P. Arnold and O. Espinosa, *Phys. Rev.* **D47**, 3546 (1993).
- [7] K. Kajantie, K. Rummukainen and M. Shaposhnikov, *Nucl. Phys.* **B407**, 356 (1993); F. Farakos, K. Kajantie, K. Rummukainen and M. Shaposhnikov, *Phys. Lett.* **B 336** 494 (1994), hep-ph/9405234; Preprint CERN-TH.7220/94 (1995); Z. Fodor, J. Hein, K. Jansen, A. Jaster, I. Montvay and F. Csikor *Phys. Lett.* **B 334**, 405 (1994), hep-lat/9405021; also hep-lat/9411052; W. Buchmüller and Z. Fodor, *Phys. Lett.* **B331**, 124 (1994).
- [8] M. Sher, *Phys. Lett.* **317B**, 159 (1993) ADDENDUM-ibid.B331:448,1994
- [9] G. Farrar and M. Shaposhnikov, *Phys. Rev. Lett.* **70**, 2833 (1993); *Phys. Rev.* **D50**, 774 (1994).



- [10] M. B. Gavela, P. Hernandez, J. Orloff and O. Pene, Mod. Phys. Lett. **9A**, 795 (1994);  
M. B. Gavela, M. Losano, J. Orloff and O. Pene, Nucl. Phys. **B430**, 345 and 382  
(1994), hep-ph/9406288 and 9406289.
- [11] P. Huet and E. Sather, Phys. Rev. **D 51**, 379 (1995), hep-ph/9404302.
- [12] S. Nasser and N. Turok, Princeton preprint PUPT-1456 (1994), hep-ph/9406270.
- [13] M. E. Shaposhnikov, JETP Lett **44**, 465 (1986); Nucl. Phys. **B287**, 757 (1987); Nucl.  
Phys. **B299**, 797 (1988).
- [14] L. McLerran, Phys. Rev. Lett. **62**, 1075 (1989).
- [15] N. Turok and J. Zadrozny, Phys. Rev. Lett. **65**, 2331 (1990).
- [16] N. Turok and J. Zadrozny, Nuc. Phys. **B 358**, 471 (1991).
- [17] L. McLerran, M. Shaposhnikov, N. Turok and M. Voloshin, Phys. Lett. **256B**, 451  
(1991).
- [18] A. Cohen, D. Kaplan and A. Nelson, Phys. Lett. **B263**, 86 (1991).
- [19] A. Cohen, D. Kaplan and A. Nelson, Nuc. Phys. **B349**, 727 (1991).
- [20] A. Cohen and D. Kaplan, Phys. Lett. **B199**, 251 (1987); Nucl. Phys. **B308**, 913  
(1988).
- [21] A. Cohen, D. Kaplan and A. Nelson, Phys. Lett. **B245**, 561 (1990).
- [22] M. Dine, P. Huet, R. Singleton and L. Susskind, Phys. Lett. **B257**, 351 (1991).
- [23] D. Comelli, M. Pietroni and A. Riotto, Nucl. Phys. **B412** (1994) 441.
- [24] M. Joyce, T. Prokopec and N. Turok, Phys. Lett. **B 339**(1994) 312 , hep-ph/9401351;  
M. Joyce, in *Electroweak Physics and the Early Universe*, eds. F. Freire and J. Romao,  
publ. Plenum, proceedings of Sintra conference, March 1994, hep-ph/9406356.

- [25] M. Dine and S. Thomas, Phys. Lett. **B 328**, 73 (1994), hep-ph/9401265.
- [26] M. Joyce, T. Prokopec and N. Turok, Princeton preprint PUPT-1496, hep-ph/9410282, Phys. Rev. **D**, to appear.
- [27] G. Giudice and M. Shaposhnikov, Phys. Lett. **B326**, 118 (1994).
- [28] K. Funakubo, A. Kakuto, S. Otsuki, K. Takenaga and F. Toyoda, Phys. Rev. **D50**, 1105 (1994); preprints hep-ph/9405422, hep-ph/9407207, hep-ph/9503495
- [29] P. Arnold and O. Espinosa, Phys. Rev. **D47**, 3546 (1993); W. Buchmüller Z. Fodor, and A. Hebecker, Phys. Lett. **B331**, 131 (1994); W. Buchmüller, Z. Fodor, T. Helbig and D. Walliser, Ann. Phys. **234**, 260 (1994), hep-ph/9303251.
- [30] N. Turok, Phys. Rev. Lett. **68**, 1803 (1992); M. Dine, R. Leigh, P. Huet, A. Linde and D. Linde, Phys. Rev. **D46**, 550 (1992); B-H. Liu, L. McLerran and N. Turok, Phys. Rev. **D46**, 2668 (1992); P. Huet, K. Kajantie, R. G. Leigh, B.-H. Liu and L. McLerran, Phys. Rev. **D48**, 2477(1993).
- [31] T. Prokopec and G. Moore, Phys. Rev. Lett. 75,777(1995) and PUP-TH-1544, LANCS-TH/9517 (1995).
- [32] E. Braaten and R. Pisarski, Phys. Rev. **D46**, 1829 (1992); Phys. Rev. **D47**, 5589 (1992); Phys. Rev. **D42**, 2156 (1990).
- [33] S. Nasser and N. Turok, in preparation.
- [34] E. M. Lifshitz and L. P. Pitaevskii, *Physical Kinetics*, Pergamon Press (1979).
- [35] We have considered only the fermion-fermion scatterings. In ref. [31] the scattering rates off gluons for quarks and off  $W$  bosons for the left-handed leptons and quarks are calculated: these contribute roughly the same amount to the scattering rate, which

reduces the diffusion constant by a factor of two relative to its value in (54). There are no such scatterings for the right-handed leptons.

- [36] J. Ambjorn, T. Askgaard, H. Porter, M. E. Shaposhnikov, Phys. Lett. **B 244**, 479 (1990); Nucl. Phys. **B 353**, 346 (1991).
- [37] S. Yu. Khlebnikov, Phys. Lett. **B300**, 376 (1993); S. Yu. Khlebnikov, Phys. Rev. **D46**, 3223 (1992).
- [38] A. G. Cohen, D. B. Kaplan and A. E. Nelson, Phys. Lett. **B294**, 57 (1992), Bulletin Board: hep-ph/9206214.
- [39] J. Cline and K. Kainulainen, preprint hep-ph/9506285.
- [40] For a discussion of phenomenological constraints see the article by I. Bigi et al. in the volume cited in [1].
- [41] J. Cline, Phys. Lett. **B338** (1994) 263, hep-ph/9405365.
- [42] V. V. Klimov, Yad. Fiz. **33**, 1734(1981); Sov. J. Nucl. Phys. **33**. 934 (1981), [Sov. Phys. JETP **55**, 199 (1982)].
- [43] H. A. Weldon, Phys. Rev. **D26**, 1394 and 2789 (1982).
- [44] J. Cline, K. Kainulainen and A. Vischer, hep-ph/9506284
- [45] E. M. Lifshitz and L. P. Pitaevskii, *Physical Kinetics*, Pergamon Press (1979).

## Figure Captions

Figure 1: Classical potential seen by a particle crossing a bubble wall. The solid line shows the mass barrier, the dashed line the effect of a  $CP$  violating condensate field on the bubble wall. For the case shown, the net barrier is monotonic and the  $WKB$  reflection of particles shows no  $CP$  violation.

Figure 2: As in Figure 1, but for the case where the net barrier is non-monotonic and the  $WKB$  reflection of particles does show  $CP$  violation.

Figure 3: ‘Decay’ processes relevant for the propagation of a chiral tau lepton asymmetry through the plasma.

Figure 4: ‘Decay’ processes relevant for the propagation of a chiral top quark asymmetry through the plasma.

Figure 5: Vector boson t-channel exchange diagrams relevant for computation of the diffusion constants of different fermion species.

This figure "fig1-1.png" is available in "png" format from:

<http://arxiv.org/ps/hep-ph/9410281v4>

This figure "fig1-2.png" is available in "png" format from:

<http://arxiv.org/ps/hep-ph/9410281v4>

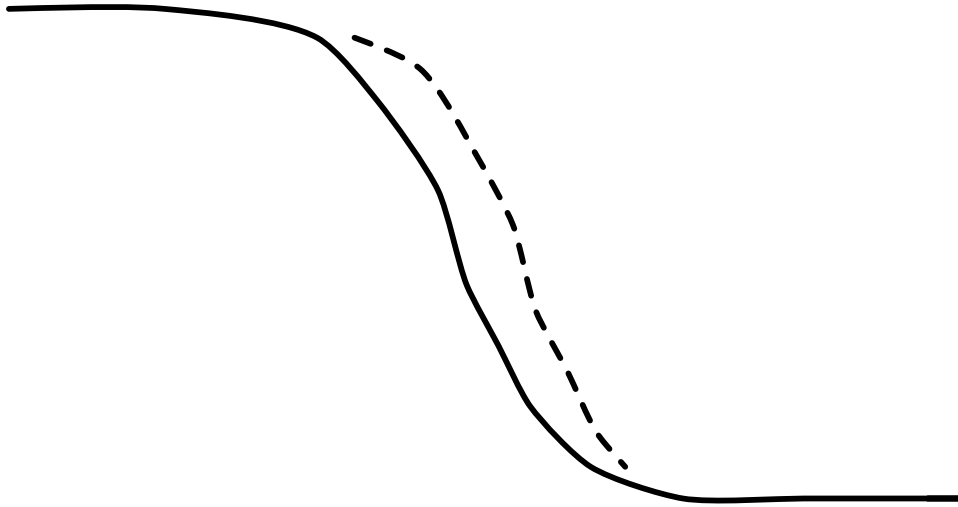


Figure 1

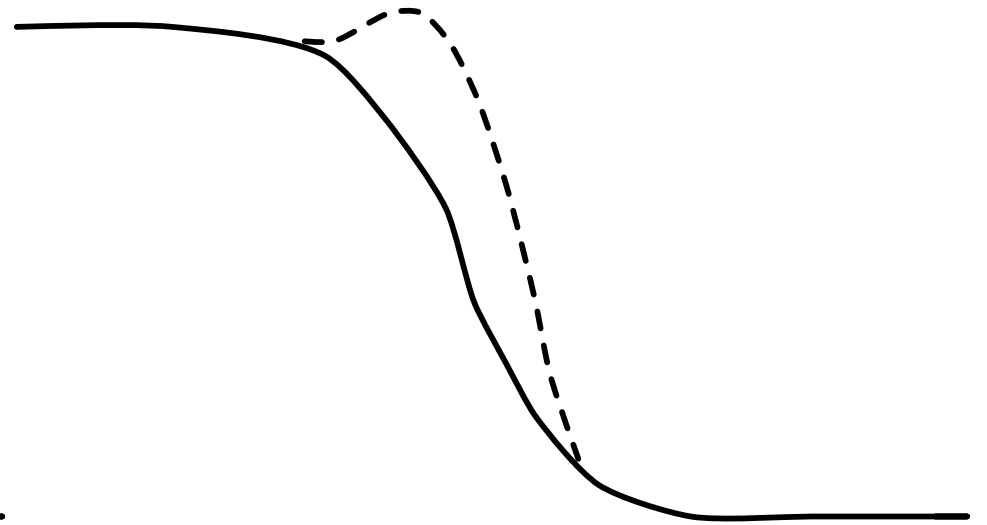


Figure 2

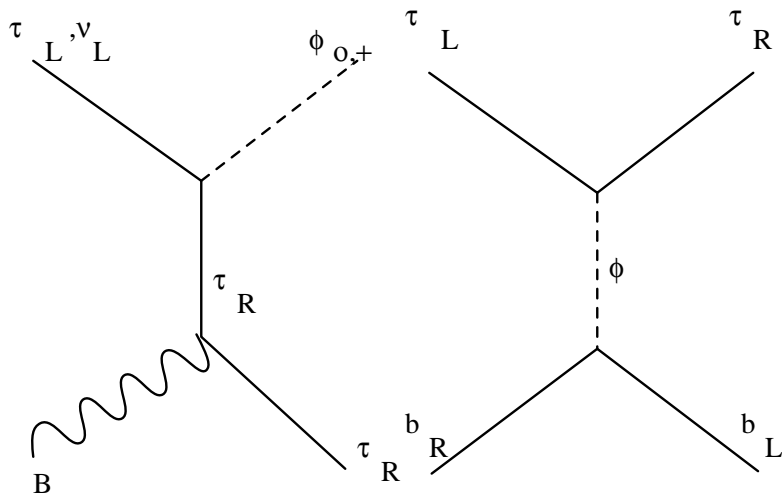


Figure 3

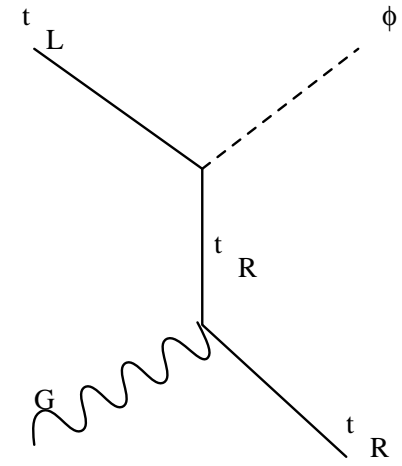


Figure 4

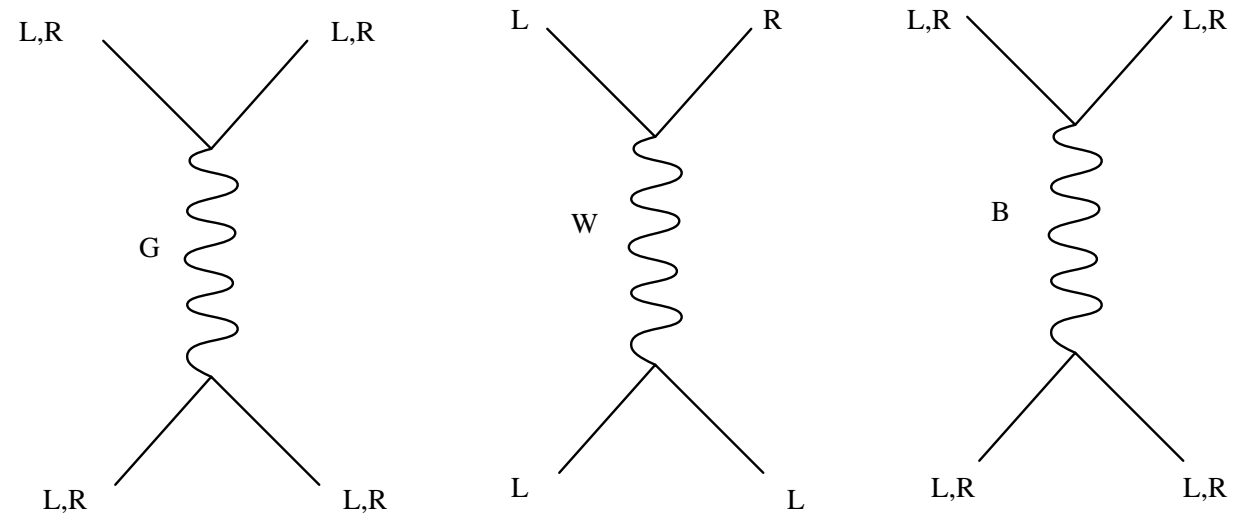


Figure 5